AIMS Mathematics, 10(9): 20157–20198.
DOI: 10.3934/math.2025901
Received: 21 June 2025
Revised: 09 August 2025
Accepted: 29 August 2025
Published: 03 September 2025

https://www.aimspress.com/journal/Math

Research article

Dynamic analysis of a fractional-order SEAIR model for influenza transmission with optimal control and stochastic stability

Hanyun Zhang, Guoqin Chen, Xingxiao Wu, Yanfang Zhao* and Yujiao Wang*

School of Mathematics and Computer Science, Yunnan Minzu University, Kunming 650500, China

* **Correspondence:** Email: zhaoyf_1979@163.com, wangyujiao5730@163.com.

Abstract: Understanding the dynamic characteristics of infectious disease transmission is key to designing effective control strategies. To this end, we proposed a Caputo fractional-order SEAIR model to study the transmission of influenza. First, the existence, uniqueness, and non-negativity of the model's solution were proven, ensuring its biological plausibility. Then, the basic reproduction number R_0 was derived using the next-generation matrix method, the existence and stability of equilibrium points were analyzed, and bifurcation phenomena in the model were proven. Next, vaccination and isolation were considered control strategies, and the existence of optimal solutions was discussed. The optimal control strategies were derived using the Pontryagin maximum principle. Through numerical simulations, the dynamic behavior of the controlled model under different initial values and η values was further analyzed. In addition, the stability of the stochastic model when $\eta = 1$ was studied, as well as the dynamic characteristics of the stochastic model under different influenza mortality rates (d). Finally, real influenza patient data was used for parameter estimation to validate the accuracy and predictive capability of the deterministic model. The research results indicated that early detection and treatment helped significantly reduce the transmission range, thereby facilitating better control of influenza. In areas with high population density, a single control strategy may not be sufficient to effectively curb the spread, thus requiring a combination of multiple strategies to achieve better control outcomes.

Keywords: fractional-order SEAIR model; basic reproduction number; stochastic stability; sensitivity analysis; optimal control
Mathematics Subject Classification: 60H25, 34A09, 92D25

1. Introduction

Influenza is an acute respiratory infectious disease caused by viruses from the Orthomyxoviridae family, primarily types A and B, which are the major pathogens responsible for seasonal influenza in

humans [1]. Typical clinical symptoms include fever, cough, and sore throat [2]. Influenza is highly contagious and has widespread effects, having caused several global pandemics throughout history, the most severe of which was the 1918 'Spanish flu,' which is estimated to have resulted in around 50 million deaths [3]. Each pandemic imposes a significant burden on public health systems and poses a major challenge to socio-economic stability [4]. Influenza not only threatens individual health but also places considerable strain on healthcare infrastructure [5]. Therefore, a comprehensive study of the biological mechanisms of influenza viruses, the development of effective vaccines and antiviral treatments, and raising public awareness of preventive measures are key strategies for mitigating the risks of future influenza pandemics.

Mathematical modeling, particularly through compartmental models, plays a crucial role in the study of influenza virus transmission dynamics. These models serve as essential quantitative tools for characterizing transmission mechanisms, forecasting epidemic trends, and evaluating intervention strategies. Building on the classical SIR model, Casagrandi et al. [6] proposed an extended SIRC model that considers individuals recovered from different influenza strains to study the epidemiological significance of antigenic drift in influenza A viruses. Their model revealed complex dynamical features, including chaotic behavior and multistable periodic outbreaks. Expanding on this, Mohammad et al. [7] integrated vaccination into their influenza model and demonstrated the significant impact of immunization on transmission dynamics. Andreu-Vilarroig et al. [8] further introduced seasonal variations and immune decline, providing in-depth insights into their effects on influenza transmission. In a broader context, Ndendya et al. [9, 10] developed a series of ODE models specifically targeting the transmission mechanisms of various infectious diseases, including rabies and conjunctivitis. Together, these models offer a multidimensional understanding of the factors influencing infectious disease spread, greatly advancing theoretical insights into epidemic transmission mechanisms.

Although ODE models have achieved significant results in influenza transmission research, they have certain limitations in capturing complex dynamics, memory effects, and nonlinear behaviors. With the development of fractional calculus, fractional-order models have become increasingly widespread in the simulation of infectious disease transmission, particularly the Caputo derivative model, which is widely used due to its compatibility with traditional initial conditions. This model can more accurately describe systems with memory effects and historical dependencies [11] and has shown unique advantages in simulating complex biological processes. Research indicates that, compared to integer-order models, fractional-order models perform better in data fitting and the precise characterization of infectious disease transmission mechanisms, providing more detailed and accurate tools for epidemic analysis and prediction [12–14].

The application of fractional-order differential equations in infectious disease modeling has made significant progress, particularly in three key areas. In the theoretical realm, Deressa et al. [15] and Soulaimani et al. [16] laid a rigorous mathematical foundation for epidemic control by conducting stability analysis based on Lyapunov functions and deriving optimal control strategies using Pontryagin's maximum principle. Moreover, Malmir [17] introduced a new fractional-order control method, expanding the application of fractional calculus in epidemic management. In terms of model development, Babrhoui et al. [18] and Zhao et al. [19] proposed innovative fractional-order SEAIR and SIDAR frameworks, providing a more accurate representation of infectious disease transmission dynamics. Furthermore, Angstmann et al. [20, 21] derived a fractional-order infectious SIR model

based on stochastic processes, which provides a new perspective for a deeper understanding of the behavior of fractional-order infectious disease models. In the domain of numerical methods, Momani et al. [22] successfully applied the Laplace residual power series method to obtain effective numerical solutions for fractional-order systems. Research findings show that fractional-order models outperform traditional integer-order models in terms of fitting accuracy and the predictive assessment of control interventions.

As research progresses, an increasing number of researchers have incorporated control measures into influenza transmission models, exploring optimal control strategies and control intensities. Lamwong et al. [23] considered isolation interventions as a control strategy and mathematically derived the control intensity that achieves the best effect with the lowest cost. Yang et al. [24] combined vaccination and antiviral treatment as a joint control strategy for influenza, and they found that early vaccination followed by treatment throughout the infection process could slow down or eradicate influenza transmission. Chen et al. [25] combined vaccination and isolation as control strategies, and their research showed that the joint implementation of both strategies resulted in the best control outcomes. Xiao et al. [26] and Moon [27] studied fractional optimal control problems with terminal and state constraints, further establishing a theoretical foundation for analyzing systems under complex conditions. Additionally, Song et al. [28] studied the conserved quantities for Hamiltonian systems on time scales, providing further theoretical support for the development of optimal control theory.

In addition, disturbances in ecosystems, such as climate change, resource fluctuations, and sudden catastrophes, can lead to changes in key parameters. To accurately describe the impact of these perturbations on system dynamics, some researchers have extended epidemic models into stochastic differential equation frameworks that incorporate environmental noise terms, enabling a more precise analysis of influenza transmission mechanisms. Farah et al. [29] developed a stochastic dual-strain influenza model that includes both resistant and non-resistant strains, and found that the decline of influenza is due to favorable environmental conditions. Su et al. [30] proposed a stochastic influenza model that combines human mobility with the Ornstein-Uhlenbeck process, exploring the impact of random factors such as population mobility on influenza transmission, and derived conditions for influenza extinction. Khan et al. [31] established a probabilistic threshold model using the stochastic basic reproduction number to systematically assess how parameter variations under different environmental scenarios affect population persistence and extinction risk. These studies provide a solid theoretical foundation for the quantitative design of ecological control strategies.

In this paper, we establish a SEAIR model based on the Caputo fractional-order calculus, aiming to explore the influenza transmission mechanisms from three aspects. First, the model reveals the complex transmission mechanisms of influenza between susceptible individuals, exposed individuals, asymptomatic infected individuals, symptomatic infected individuals, and recovered individuals, and analyzes the impact of key parameters on the transmission. Second, we discuss influenza control strategies such as vaccination and quarantine, simulate the effects of intervention measures during an epidemic, and evaluate the optimal control strategies. Finally, using the model, we consider the impact of random factors on influenza transmission, further deepening the understanding of transmission dynamics. In this study, we aim to provide a theoretical foundation for epidemic control and offer scientific insights for optimizing intervention strategies.

The chapters of this paper are organized as follows: In Section 2, we introduce the construction of the Caputo fractional-order SEAIR model. In Section 3, we analyze the complex dynamics of the

model. In Section 4, we explore the optimization strategy when immune vaccination and isolation are used as control measures and derive the optimal solution. In Section 5, we examine the stochastic stability of the model at equilibrium. In Section 6, we perform parameter estimation and curve fitting using real data. In Section 7, we summarize the major conclusions.

2. Establishing model structure and preliminary concepts

2.1. Establishing model structure

In 2021, Basnarkov [32] proposed a SEAIR epidemic model, namely,

$$\begin{aligned} &\dot{S}(t) = -aAS - \beta IS, \quad \dot{E}(t) = aAS + \beta IS - \delta E, \\ &\dot{A} = \delta E - pA - qA, \quad \dot{I} = pA - \nu I, \quad \dot{R} = qA + \nu I, \end{aligned} \tag{2.1}$$

where $S(t)$, $E(t)$, $A(t)$, $I(t)$, and $R(t)$ represent susceptible, exposed, asymptomatic, symptomatic, and recovered individuals, respectively. The contact rate between asymptomatic carriers and susceptibles is a. Other parameters are defined in Table 1.

Table 1. Definitions of parameters in model (2.2).

Parameter	Definition
Λ	The constant input of population
β	Effective contact rate
α	Infection suppression coefficient
d	Population mortality rate
σ	The transition rate of recovered individuals back to the susceptible
δ	The proportion of exposed individuals who become infected
k	The proportion of asymptomatic individuals among those exposed who become infected
q	Asymptomatic-to-recovered transition rate
ν	The rate at which symptomatic infections transition to recovered states
u	Illness and death rates among individuals presenting symptoms due to infection
p	The incidence of transitioning from asymptomatic to symptomatic infection status

Based on model (2.1), we consider the following points:

- Population mobility and the birth of new individuals affect the total population dynamics.
- Considering that the time for asymptomatic carriers to transition to symptomatic carriers is short, and that asymptomatic carriers have a low viral load with their immune system effectively controlling the virus, resulting in a lower transmission rate, we therefore neglect the transmission impact of asymptomatic carriers on susceptible individuals.
- When symptomatic individuals come into contact with susceptible individuals, the susceptible individuals become exposed. With the rise in symptomatic cases, preventive strategies like mask usage and home confinement play a key role in minimizing transmission risk. Therefore, using $\beta SI/(1 + \alpha I)$ with a saturation effect to describe the impact of symptomatic individuals on susceptible individuals is more reasonable [15].

- All groups face the same natural death risk.
- Traditional ODE models struggle to capture the hereditary and memory effects of infectious diseases, while the Caputo fractional-order model can more accurately handle these characteristics, overcoming the limitations of traditional models [33].

Therefore, we developed the following Caputo fractional-order SEAIR model for infectious disease transmission

$$\begin{cases} {}^{C}D_t^{\eta}S(t) = \Lambda - \frac{\beta S I}{1+\alpha I} - dS + \sigma R, \\ {}^{C}D_t^{\eta}E(t) = \frac{\beta S I}{1+\alpha I} - (\delta + d)E, \\ {}^{C}D_t^{\eta}A(t) = k\delta E - (p + q + d)A, \\ {}^{C}D_t^{\eta}I(t) = (1-k)\delta E + pA - (\nu + d + u)I, \\ {}^{C}D_t^{\eta}R(t) = qA + \nu I - (\sigma + d)R. \end{cases} \tag{2.2}$$

The schematic diagram of the influenza model (2.2) is shown in Figure 1, and the parameter definitions are provided in Table 1. The model (2.2) is a Caputo fractional-order influenza model that captures nonlocality and memory effects, effectively describing history-dependent features of influenza, such as latency and immune delay. Clearly, when $\eta = 1$, model (2.2) reduces to a ODE influenza model, which indicates that the fractional-order influenza model is more flexible in characterizing the transmission mechanism of influenza and can more accurately predict the trends of influenza spread.

In Figure 1, susceptible individuals S maintain a constant total population input Λ. Some susceptible individuals, after effective contact with symptomatic infectives I, transition to the exposed class E, a process governed by the saturated infection rate $\frac{\beta I}{1+\alpha I}$. As the virus spreads, exposed individuals transition into infected classes, including asymptomatic individuals A and symptomatic individuals I. Asymptomatic individuals A either transition to symptomatic individuals I or directly to recovered individuals, depending on their immunity. On the other hand, symptomatic individuals I may either die due to severe illness or recover through timely medical treatment. Recovered individuals, although healthy, may revert to susceptible individuals due to a weakening immune system. A certain proportion of natural deaths occur within each group.

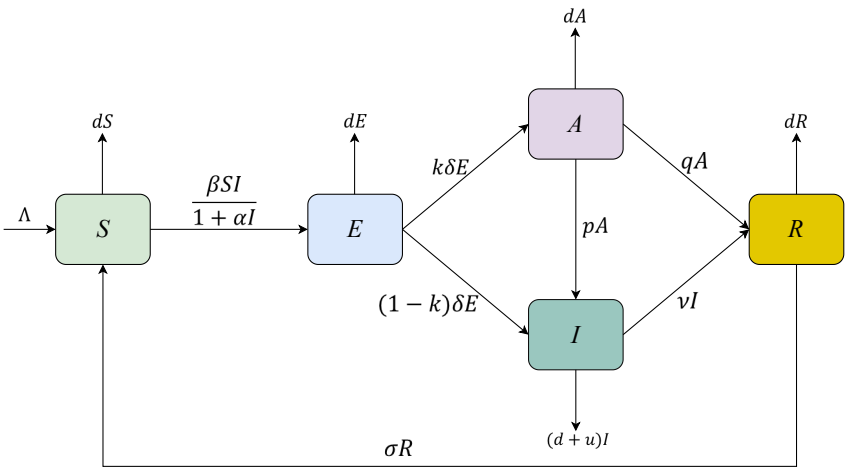

Figure 1. Flow chart of SEAIR transmission.

2.2. Preliminary concepts

Definition 2.1 ([34]). *Let $f : \mathbb{C}^n[t_0, \infty) \to \mathbb{R}$ and its fractional Caputo derivative of order $\eta > 0$ is defined as*

$$D^{\eta} f(t) = \frac{1}{\Gamma(n-\eta)} \int_{t_0}^{t} \frac{f^{(n)}(\tau)}{(t-\tau)^{\eta-n+1}} d\tau,$$

where the set of n-times continuously differentiable functions on the interval $[t_0, \infty)$, denoted as $\mathbb{C}^n[t_0, \infty)$, uses the Gamma function $\Gamma(n)$. Here, $n \in \mathbb{N}^+$ such that $n-1 < \eta < n$, with $t > t_0$. When $0 < \eta < 1$, the definition of the function takes a distinct form

$$D^{\eta} f(t) = \frac{1}{\Gamma(1-\eta)} \int_{t_0}^{t} \frac{f'(\tau)}{(t-\tau)^{\eta}} d\tau.$$

Lemma 2.1 ([35]). *For $f \in \mathbb{C}^1[a, b]$ and α within the interval (0, 1].*
(i) For all $t \in [a, b]$ with $D^{\alpha} f(t) \geq 0$, $f(t)$ exhibits monotonic non-decreasing behavior.
(ii) If $D^{\alpha} f(t) \leq 0$ holds true for every $t \in [a, b]$, $f(t)$ exhibits monotonic ascent.

Lemma 2.2 ([36]). *Let $x : [t_0, \infty) \to \mathbb{R}$ be a continuous function that satisfies*

$$\begin{cases} D^{\alpha} x(t) + \lambda x(t) \leq \mu, \\ x(t_0) = x_0, \end{cases} \tag{2.3}$$

where $\alpha \in (0, 1], \lambda, \mu \in \mathbb{R}, \lambda \neq 0$ and $t_0 \geq 0$ is the initial time. Then we obtain

$$x(t) \leq \left(x_0 - \frac{\mu}{\lambda}\right) E_{\alpha}\left[-\lambda (t-t_0)^{\alpha}\right] + \frac{\mu}{\lambda}.$$

Lemma 2.3 ([37]). *Let us examine a polynomial expression*

$$P(x) = x^n + c_1 x^{n-1} + c_2 x^{n-2} + \cdots + c_n = 0. \tag{2.4}$$

The criteria ensuring all roots of (2.4) meet

$$|arg(x)| > \frac{\eta\pi}{2} \tag{2.5}$$

are:

- *With $n = 1$, the prerequisite for condition (2.4) is that c_1 must exceed zero.*
- *For $n = 2$, (2.5) is met if the Routh-Hurwitz criteria are met or if c_1 is negative and $4c_2$ exceeds $\frac{c_1^2}{2}$.*
- *For $n = 3$, if $D(P) > 0$, the Routh-Hurwitz criteria $c_1, c_3 > 0$ and $c_1 c_2 > c_3$ are both necessary and sufficient for (2.5). When the discriminant $D(P)$ is negative, two scenarios emerge:*
  - *If $c_1 \geq 0$, $c_2 \geq 0$, and $c_3 > 0$, along with $\eta < \frac{2}{3}$, then inequality (2.5) is satisfied.*
  - *Conversely, if $c_1 < 0$ and $c_2 < 0$, while $\eta > \frac{2}{3}$, every root of $P(x) = 0$ will meet the inequality $|\arg(x)| < \frac{\eta\pi}{2}$.*

  If $D(P) < 0$, $c_1, c_2 \geq 0$ and $c_1 c_2 = c_3$, (2.5) holds when $\eta \in [0, 1)$.

- *For all n, c_n must be positive as a prerequisite for (2.5).*

Lemma 2.4 ([39]). *Examine the following fractional-order model*

$$D^{\eta}z(t) = g(t, z), z(t_0) = z_0 \text{ and } t_0 > 0, \tag{2.6}$$

where $\eta \in (0, 1]$ and $g : [t_0, \infty) \times \Omega \to \mathbb{R}^n$. If $g(t, z)$ in Eq (2.6) satisfies the local Lipschitz condition in z, then (2.6) exists a unique solution on $[t_0, \infty) \times \Omega$.

3. Dynamical analysis of model (2.2)

Before analyzing the dynamics of model (2.2), it is necessary to verify the existence, uniqueness, non-negativity, and boundedness of its solutions to ensure the biological relevance of model (2.2).

3.1. Existence and uniqueness of the solution

Theorem 3.1. *The model (2.2) has a unique solution at each time point $t > t_0$, for any initial condition $X_{t_0} = (S_{t_0}, E_{t_0}, A_{t_0}, I_{t_0}, R_{t_0}) \in \Omega$.*

Proof. Take $Y = (S, E, A, I, R)$, $Z = (S_1, E_1, A_1, I_1, R_1) \in \Omega$. We consider the function $H : \Omega \to \mathbb{R}^5$, where

$$H(X) = (H_1(X), H_2(X), H_3(X), H_4(X), H_5(X))$$

and

$$\begin{aligned}
H_1(X) &= \Lambda - \tfrac{\beta S I}{1+\alpha I} - dS + \sigma R,\\
H_2(X) &= \tfrac{\beta S I}{1+\alpha I} - (\delta + d)E,\\
H_3(X) &= k\delta E - (p + q + d)A,\\
H_4(X) &= (1 - k)\delta E + pA - (\nu + d + u)I,\\
H_5(X) &= qA + \nu I - (\sigma + d)R.
\end{aligned}$$

For all $Y, Z \in \Omega$, it holds that

$$\begin{aligned}
\|H(Y) - H(Z)\| &= |-(\frac{\beta S I}{1+\alpha I} - \frac{\beta S_1 I_1}{1+\alpha I_1}) - d(S - S_1) + \sigma(R - R_1)| + |(\frac{\beta S I}{1+\alpha I} - \frac{\beta S_1 I_1}{1+\alpha I_1})\\
&\quad - (\delta + d)(E - E_1)| + |k\delta(E - E_1) - (p + q + d)(A - A_1)|\\
&\quad + |(1 - k)\delta(E - E_1) + p(A - A_1) - (\nu + d + u)(I - I_1)|\\
&\quad + |q(A - A_1) + \nu(I - I_1) - (\delta + d)(R - R_1)|\\
&\le 2\beta|S I - S_1 I_1| + d|S - S_1| + \sigma|R - R_1| + (\delta + d)|E - E_1| + k\delta|E - E_1|\\
&\quad + (p + q + d)|A - A_1| + (1 - k)\delta|E - E_1| + p|A - A_1| + (\nu + d + u)|E - E_1|\\
&\quad + q|A - A_1| + \nu|I - I_1| + (\sigma + d)|R - R_1|\\
&\le \alpha|S - S_1| + (2\sigma + d)|R - R_1| + (2\delta + d)|E - E_1| + (2p + 2q + d)|A - A_1|\\
&\quad + (2\nu + d + u)|I - I_1| + 2Q_2\beta[|S - S_1| + |I - I_1|]\\
&\le (d + 2Q_2\beta)|S - S_1| + (2\sigma + d)|R - R_1| + (2\delta + d)|E - E_1|\\
&\quad + (2p + 2q + d)|A - A_1| + (2\nu + d + u + 2Q_2\beta)|I - I_1|\\
&\le K\|Y - Z\|.
\end{aligned}$$

Based on the upper bounds of the Lipschitz constants for the individual equations in the system, the overall constant is obtained

$$K = \max\{d + 2Q_2\beta, 2\sigma + d, 2\delta + d, 2p + 2q + d, 2\nu + d + u + 2Q_2\beta\}.$$

Therefore, for any $X, Y \in \Omega$, we have

$$\|H(X) - H(Y)\| \leq K \|X - Y\|.$$

This implies that $H(X)$ satisfies the local Lipschitz's condition on $[0, +\infty) \times \Omega$. By Lemma 2.4, model (2.2) has a unique solution for any given initial condition $X_{t_0} \in \Omega$. □

3.2. Non-negativity and boundedness solutions

To ensure the stability and viability of the solutions to the model, the population sizes must remain strictly positive and within a bounded region. Therefore, the set $\Omega^+ = \{(S, E, A, I, R) \in \Omega \mid S > 0, E > 0, A > 0, I > 0, R > 0\}$ is defined to represent the solutions of model (2.2) that satisfy the non-negativity and boundedness constraints.

Theorem 3.2. *For $t > 0$, each solution of model (2.2) initiated in Ω^+ remains non-negative.*

Proof. Let $X_{t_0} = (S_{t_0}, E_{t_0}, A_{t_0}, I_{t_0}, R_{t_0}) \in \Omega^+$ be the initial condition for model (2.2). Based on model (2.2), we obtain

$$D^\eta S\Big|_{S_{t_0}=0} = \Lambda + \sigma R > 0, \; D^\eta E\Big|_{E_{t_0}=0} = \frac{\beta S I}{1 + \alpha I} \geq 0,$$

$$D^\eta A\Big|_{I_{t_0}=0} = k\delta E \geq 0, \; D^\eta I\Big|_{I_{t_0}=0} = (1 - k)\delta E + pA \geq 0, \; D^\eta R\Big|_{R_{t_0}=0} = qA + \nu I \geq 0.$$

According to Lemma 2.1, for $t \geq t_0$, $S(t) > 0$, $E(t) > 0$, $A(t) > 0$, $I(t) > 0$, and $R(t) > 0$. Therefore, under the constraints of Ω^+, the solutions of model (2.2) will always remain within Ω^+. Next, define

$$N(t) = S(t) + E(t) + A(t) + I(t) + R(t)$$

and

$$\begin{aligned} D^\eta N &= D^\eta S + D^\eta E + D^\eta A + D^\eta I + D^\eta R = \Lambda - dN - uI, \\ &\Rightarrow D^\eta N + dN + uI = \Lambda, \\ &\Rightarrow D^\eta N + dN \leq \Lambda. \end{aligned}$$

By Lemma 2.2, as $t \to \infty$, we have

$$\lim_{t\to\infty} N(t) = \left(N(t_0) - \frac{\Lambda}{d}\right) E_\alpha\left[-d(t - t_0)\right] + \frac{\Lambda}{d}.$$

The solution of the model (2.2) for X_{t_0} will always remain within Ω and satisfy $0 \leq S + E + A + I + R \leq \frac{\Lambda}{d}$. □

The above analysis shows that model (2.2) is biologically meaningful. Next, we explore the dynamical characteristics of model (2.2).

3.3. Basic reproduction number

The basic reproduction number [38] R_0 represents the average number of new infections that a single infected individual may cause in a susceptible population. It is an important indicator for assessing whether a disease will spread or decline. Specifically, if $R_0 < 1$, the disease will disappear from the population; if $R_0 > 1$, the disease will continue to spread within the population. Next, the next-generation matrix method [40] is utilized for calculating R_0. Let

$$\phi = \begin{bmatrix} \frac{\beta S I}{1+\alpha I} \\ (1-k)\delta E \\ qA + \nu I \end{bmatrix}, \psi = \begin{bmatrix} (\delta + d)E \\ (p + q + d)A \\ (\nu + d + u)I \end{bmatrix}.$$

The model (2.2) reaches an optimal condition known as the disease-free equilibrium (DFE) $P_0 = \left(\frac{\Lambda}{d}, 0, 0, 0, 0\right)$. At this stable state, the model shows no signs of infection. Accordingly, the Jacobian matrices for the functions ϕ and ψ evaluated at P_0 take the following form

$$F = \begin{bmatrix} 0 & 0 & \beta\frac{\Lambda}{d} \\ (1-k)\delta & 0 & 0 \\ 0 & q & \nu \end{bmatrix}, V = \begin{bmatrix} \delta + d & 0 & 0 \\ 0 & p + q + d & 0 \\ 0 & 0 & \nu + d + u \end{bmatrix}.$$

The R_0 of model (2.2) is defined as

$$FV^{-1} = \begin{bmatrix} 0 & 0 & \frac{\beta\Lambda}{d(\nu+d+u)} \\ \frac{(1-k)\delta}{\delta+d} & 0 & 0 \\ 0 & \frac{q}{p+q+d} & \frac{\nu}{\nu+d+u} \end{bmatrix},$$

thus, $R_0 = \frac{\beta\Lambda}{d(\nu+d+u)}$.

The basic reproduction number R_0 plays a critical role in the spread of influenza. When $R_0 < 1$, the influenza will gradually decline, while when $R_0 > 1$, it may outbreak. However, whether an outbreak occurs also depends on other key factors. To better understand this process, we conducted a numerical simulation to study the impact of different d values on R_0 under fixed ν and u, as well as the effects of parameters Λ and β. The results are shown in Figure 2. The analysis indicates that as Λ and β increase, R_0 also increases. Furthermore, as d increases, the values of Λ and β at $R_0 = 1$ also rise. This suggests that moderately increasing the natural mortality rate of the population helps to control influenza spread. However, our goal is to control the spread of influenza while minimizing natural mortality, which requires reducing Λ and β values by reducing inter-regional movement and lowering contact between susceptible individuals and infected persons.

To determine the internal equilibria of the model (2.2), we define

$$\begin{cases} \Lambda - \frac{\beta S I}{1+\alpha I} - dS + \sigma R = 0, \\ \frac{\beta S I}{1+\alpha I} - (\delta + d)E = 0, \\ k\delta E - (p + q + d)A = 0, \\ (1-k)\delta E + pA - (\nu + d + u)I = 0, \\ qA + \nu I - (\sigma + d)R = 0. \end{cases} \tag{3.1}$$

Solving Eq (3.1) yields Theorem 3.3.

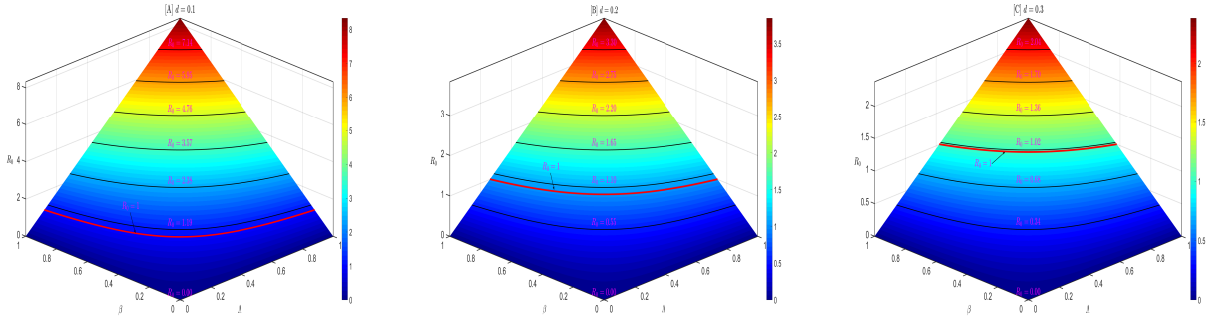

Figure 2. The impact of changes in parameters Λ and β on R_0, with $\nu = 0.5$ and $u = 0.6$ fixed.

Theorem 3.3. *If*

$$R_0 > (\delta + d)(p + q + d)/\delta(p + q + d - kq - kd) > 1,$$

then model (2.2) has an endemic equilibrium (EE) $P_* = (S^*, E^*, A^*, I^*, R^*)$.

Proof. Based on the second equation of Eq (3.1), we have

$$E = \frac{\beta S I}{(\delta + d)(1 + \alpha I)}. \tag{3.2}$$

Similarly, the third equation of Eq (3.1) leads to

$$E = \frac{p + q + d}{k\delta} A, \tag{3.3}$$

thus,

$$\frac{\beta S I}{(\delta + d)(1 + \alpha I)} = \frac{p + q + d}{k\delta} A. \tag{3.4}$$

Furthermore, by combining the third and fourth equations of Eq (3.1), it can be obtained that

$$\delta E - (q + d) A - (\nu + d + u) I = 0. \tag{3.5}$$

Substituting (3.2) into (3.5) gives

$$A = \frac{\delta\beta S I}{(q + d)(\delta + d)(1 + \alpha I)} - \frac{\nu + d + u}{q + d} I. \tag{3.6}$$

Similarly, substituting (3.6) into (3.4) yields

$$S = \frac{(\delta + d)(p + q + d)(\nu + d + u)(1 + \alpha I)}{\delta\beta(p + q + d - kq - kd)}. \tag{3.7}$$

Additionally, by combining the first and fifth equations of Eq (3.1), we get

$$\Lambda - \frac{\beta S I}{1 + \alpha I} - dS + \frac{\sigma q k \delta \beta S I}{(p + q + d)(\sigma + d)(\delta + d)(1 + \alpha I)} + \frac{\sigma \nu I}{\sigma + d} = 0. \tag{3.8}$$

Substituting (3.7) into (3.8), we can derive

$$I^* = \frac{\Lambda - M_4}{M_1 - M_2 - M_3},$$

where

$$M_1 = \frac{(\beta + d\alpha)(\delta + d)(p + q + d)(\nu + d + u)}{\delta\beta(p + q + d - kq - kd)}, \quad M_2 = \frac{\sigma qk(\nu + d + u)}{(\sigma + d)(p + q + d - kq - kd)},$$

$$M_3 = \frac{\sigma\nu}{\sigma + d}, \quad M_4 = \frac{d(\delta + d)(p + q + d)(\nu + d + u)}{\delta\beta(p + q + d - kq - kd)}.$$

To ensure biological significance, $I^* > 0$, which means

$$(M_1 - M_2 - M_3)(\Lambda - M_4) > 0.$$

Let $M = M_1 - M_2 - M_3$, then

$$\begin{aligned} M &= \frac{M_5}{\delta\beta(\sigma + d)(p + q + d - kq - kd)} \\ &= \frac{[(\sigma + d)(\beta + d\alpha)(\delta + d)(p + q + d) - \delta\beta\sigma qk](\nu + d + u) - \sigma\nu\delta\beta(p + q + d - kq - kd)}{\delta\beta(\sigma + d)(p + q + d - kq - kd)}. \end{aligned}$$

This means that the sign of M is determined by M_5. Since

$$\begin{aligned} M_5 &= \nu\left(\sigma\delta d\alpha + \delta d\beta + d^2\alpha\delta + \sigma d\beta + \sigma d^2\alpha + d^2\beta + d^3\alpha\right) + \sigma\delta\beta kd\nu - \sigma\delta\beta kq(d + u) \\ &\quad + q\left(\sigma\delta\beta + \sigma\delta d\alpha + \delta d\beta + d^2\alpha\delta + \sigma d\beta + \sigma d^2\alpha + d^2\beta + d^3\alpha\right)(d + u) \\ &\quad + \left(\sigma\delta\beta + \sigma\delta d\alpha + \delta d\beta + d^2\alpha\delta + \sigma d\beta + \sigma d^2\alpha + d^2\beta + d^3\alpha\right)(d + u)(p + d) \\ &\geq \nu\left(\sigma\delta d\alpha + \delta d\beta + d^2\alpha\delta + \sigma d\beta + \sigma d^2\alpha + d^2\beta + d^3\alpha\right) + \sigma\delta\beta d\nu - \sigma\delta\beta q(d + u) \\ &\quad + q\left(\sigma\delta\beta + \sigma\delta d\alpha + \delta d\beta + d^2\alpha\delta + \sigma d\beta + \sigma d^2\alpha + d^2\beta + d^3\alpha\right)(d + u) \\ &\quad + \left(\sigma\delta\beta + \sigma\delta d\alpha + \delta d\beta + d^2\alpha\delta + \sigma d\beta + \sigma d^2\alpha + d^2\beta + d^3\alpha\right)(d + u)(p + d) \\ &\geq \nu\left(\sigma\delta d\alpha + \delta d\beta + d^2\alpha\delta + \sigma d\beta + \sigma d^2\alpha + d^2\beta + d^3\alpha\right) + \sigma\delta\beta d\nu \\ &\quad + q\left(\sigma\delta d\alpha + \delta d\beta + d^2\alpha\delta + \sigma d\beta + \sigma d^2\alpha + d^2\beta + d^3\alpha\right)(d + u) \\ &\quad + \left(\sigma\delta\beta + \sigma\delta d\alpha + \delta d\beta + d^2\alpha\delta + \sigma d\beta + \sigma d^2\alpha + d^2\beta + d^3\alpha\right)(d + u)(p + d) \\ &> 0. \end{aligned}$$

This indicates that $M > 0$. Therefore, $\Lambda > M_4$, i.e.,

$$R_0 > \frac{(\delta + d)(p + q + d)}{\delta(p + q + d - kq - kd)} = \phi > 1. \tag{3.9}$$

When Eq (3.9) holds, we can derive

$$S^* = N(1 + \alpha I^*), \quad E^* = \frac{\beta S^* I^*}{(\delta + d)(1 + \alpha I^*)},$$

$$A^* = \frac{k\delta\beta S^* I^*}{(\delta + d)(p + q + d)(1 + \alpha I^*)}, \quad R^* = \frac{\beta S^* I^*}{\sigma(1 + \alpha I^*)} + \frac{dS^* - \Lambda}{\sigma}.$$

Obviously, $S^* > 0$, $E^* > 0$ and $A^* > 0$ hold. From $R^* > 0$, we have

$$\frac{\Lambda - M_4}{M_1 - M_2 - M_3} > \frac{\Lambda - M_4}{M_1}. \tag{3.10}$$

Through simple calculation, it can be concluded that Eq (3.10) holds, i.e., $R^* > 0$. Based on the above analysis, if Eq (3.9) holds, model (2.2) has an internal equilibrium P^*. □

3.4. Stability of the equilibria

To analyze the model (2.2), we next examine its stability at P_0 and P^*. The Jacobian matrix of model (2.2) is

$$J(S, E, A, I, R) = \begin{bmatrix} -\frac{\beta I}{1+\alpha I} - d & 0 & 0 & -\frac{\beta S}{(1+\alpha I)^2} & \sigma \\ \frac{\beta I}{1+\alpha I} & -(\delta + d) & 0 & \frac{\beta S}{(1+\alpha I)^2} & 0 \\ 0 & k\delta & -(p + q + d) & 0 & 0 \\ 0 & (1-k)\delta & p & -(\nu + d + u) & 0 \\ 0 & 0 & q & \nu & -(\sigma + d) \end{bmatrix}.$$

Theorem 3.4. *The DFE P_0 of model (2.2) is locally asymptotically stable, provided that $R_0 < \phi$ (see Figure 3).*

Proof. The Jacobian at P_0 is

$$J(P_0) = \begin{bmatrix} -d & 0 & 0 & -\frac{\beta\Lambda}{d} & \sigma \\ 0 & -(\delta + d) & 0 & \frac{\beta\Lambda}{d} & 0 \\ 0 & k\delta & -(p + q + d) & 0 & 0 \\ 0 & (1-k)\delta & p & -(\nu + d + u) & 0 \\ 0 & 0 & q & \nu & -(\sigma + d) \end{bmatrix}.$$

The calculation yields that $J(P_0)$ has two eigenvalues, i.e., $\lambda_1 = -d$ and $\lambda_2 = -(d+\sigma)$, whose arguments are greater than $\frac{\eta\pi}{2}$. Additionally, the remaining eigenvalues of the matrix $J(P_0)$, denoted as λ_i $(i = 3, 4, 5)$, can be obtained from the eigenvalues of the matrix

$$J_1 = \begin{bmatrix} -(\delta + d) & 0 & \frac{\beta\Lambda}{d} \\ k\delta & -(p + q + d) & 0 \\ (1-k)\delta & p & -(\nu + d + u) \end{bmatrix}.$$

The characteristic equation is $\lambda^3 + a_1\lambda^2 + a_2\lambda + a_3 = 0$, where

$$\begin{aligned} a_1 &= \delta + 3d + p + q + \nu + u > 0, \\ a_2 &= (\delta + d)(\nu + d + u) + (p + q + d)[(\delta + d) + (\nu + d + u)] + \frac{\beta\Lambda\delta}{d}(1 - k) > 0, \\ a_3 &= (\delta + d)(p + q + d)(\nu + d + u) + \frac{\beta\Lambda\delta}{d}(q + d)(k - 1) - \frac{\beta\Lambda\delta p}{d} \\ &= (\delta + d)(p + q + d)(\nu + d + u) + R_0\delta(\nu + d + u)[(q + d)(k - 1) - p] \\ &= (\nu + d + u)(\delta + d)(p + q + d) + R_0\delta[(q + d)(k - 1) - p]. \end{aligned}$$

Considering the Routh–Hurwitz criteria applied to fractional differential equations as per [41], it follows that $|\arg(\lambda_i)| > \frac{\eta\pi}{2}$ $(i = 3, 4, 5)$. Consequently, all stability criteria are satisfied, confirming that under $\eta \in (0, 1)$ and

$$R_0 < \frac{(\delta + d)(p + q + d)}{\delta[(q + d)(1 - k) + p]} = \phi,$$

the DFE P_0 is locally stable. □

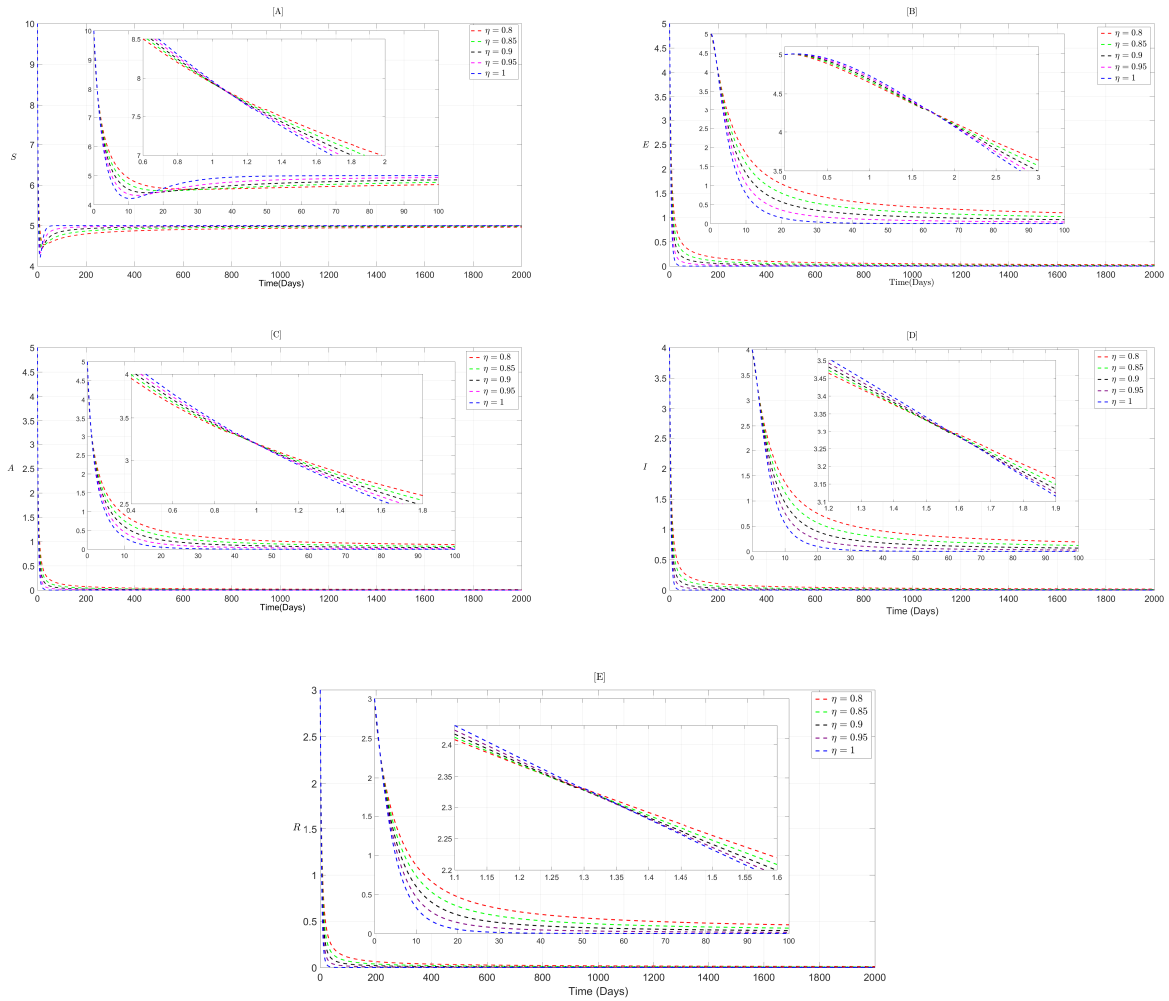

Figure 3. The dynamic behavior of model (2.2) when $1 < R_0 < \phi$. Parameters: $\Lambda = 1$, $\beta = 0.2$, $\alpha = 0.3$, $d = 0.2$, $\sigma = 0.7$, $\delta = 0.5$, $k = 0.4$, $p = 0.3$, $q = 0.2$, $\nu = 0.3$, and $u = 0.3$.

Remark 3.1. *According to Theorem 3.4, when $R_0 < \phi$, within a certain neighborhood of the DFE P_0, the flu will naturally fade away without the need for control measures.*

Theorem 3.5. *The equilibrium P^* is locally asymptotically stable when $d_1, d_2, d_3, d_4, d_5 > 0$.*

Proof. The Jacobian at P^* is

$$J(P^*) = \begin{bmatrix} -\theta_1 - d & 0 & 0 & -\theta_2 & \sigma \\ \theta_1 & -(\delta + d) & 0 & \theta_2 & 0 \\ 0 & k\delta & -(p + q + d) & 0 & 0 \\ 0 & (1-k)\delta & p & -(\nu + d + u) & 0 \\ 0 & 0 & q & \nu & -(\sigma + d) \end{bmatrix},$$

where

$$\theta_1 = \frac{\beta I^*}{1 + \alpha I^*}, \ \ \theta_2 = \frac{\beta S^*}{(1 + \alpha I^*)^2}.$$

Thus, the characteristic equation is $\lambda^5 + d_1\lambda^4 + d_2\lambda^3 + d_3\lambda^2 + d_4\lambda + d_5 = 0$, where

$$\begin{aligned}
d_1 &= 2Q_1 + Q_2 + Q_3 + \theta_1 + d, \\
d_2 &= Q_1Q_2 + Q_1Q_3 + Q_2Q_3 + Q_1 + (Q_1 + 1)(\theta_1 + d) - \theta_2(1-k)\delta, \\
d_3 &= Q_1Q_2Q_3 + \theta_2 k\delta p + Q_1(\theta_1 + d)(Q_1 + Q_2 + Q_3) - \theta_2(1-k)\delta(\theta_1 + Q_1 + d), \\
d_4 &= (\theta_1 + Q_1 + d)(Q_1Q_2 + Q_1Q_3 + Q_2Q_3 + Q_1 + d)[Q_1Q_2Q_3 + \theta_2 k\delta p - Q_2\theta_2\delta] \\
&\quad + Q_1(\theta_1 + d)(Q_1Q_2 + Q_1Q_3 + Q_2Q_3) + (1-k)\delta\theta_1\theta_2Q_1 - \theta_2(1-k)\delta, \\
d_5 &= Q_1Q_2Q_3 - Q_2\theta_2(1-k)\delta + (1-k)\delta Q_2\theta_1\theta_2, \\
Q_1 &= \delta + d, Q_2 = p + q + d, Q_3 = \nu + d + u, Q_4 = \sigma + d.
\end{aligned}$$

Remark 3.2. *Theorems 3.3 and 3.5 indicate that when $d_1 > 0$, $d_2 > 0$, $d_3 > 0$, $d_4 > 0$, $d_5 > 0$, and $R_0 > (\delta + d)(p + q + d)/\delta(p + q + d - kq - kd)$, if no control measures are taken, the flu will outbreak, and eventually, the five groups will coexist.*

Next, applying Lemma 2.3, we establish P^* is locally asymptotically stable provided that d_1, d_2, d_3, d_4 and d_5 are positive. □

To analyze the global stability of P_0 and P^*, we present Lemma 3.1.

Lemma 3.1 ([42]). *Consider $\Re$ as a compactly enclosed subset. For every solution to $Dx(t) = h(t, x)$, beginning in $\Re$, stays in $\Re$ for all time. Additionally, suppose $u(x) : \Re \to \mathbb{R}$ is a continuous function satisfying $Du(x) \leq 0$. Consider the maximal invariant set $\mathfrak{M}$ defined by $\{x \mid Du(x) = 0\}$. It follows that any trajectory $x(t)$ starting within $\Re$ converges to $\mathfrak{M}$ as $t \to \infty$. Furthermore, if $\mathfrak{M}$ reduces to the singleton $\{0\}$, then $x(t)$ asymptotically approaches zero over time.*

Lemma 3.2 ([39]). *For any $\Phi \in \mathbb{R}$ with continuous differentiability of order η, where $0 < \eta < 1$, the result holds true for all $t > t_0$.*

$$D^\eta\left[\Phi(t) - \Psi\left(1 + \ln\frac{\Phi(t)}{\Psi}\right)\right] \leq \left(1 - \frac{\Psi}{\Phi(t)}\right)D^\eta\Phi(t).$$

Theorem 3.6. *If $R_0 < 1$, P_0 is globally asymptotically stable for model (2.2).*

Proof. For analyze the global asymptotic stability of P_0, we define the Lyapunov function as

$$\mathcal{L}_1(S, E, A, I, R) = E + A + I. \tag{3.11}$$

It is evident that $\mathcal{L}_1$ is positive definite when $S,\ E,\ A,\ I,\ R \in \mathbb{R}^+$.

$$\begin{aligned} D^\eta \mathcal{L}_1(S,E,A,I,R) &= D^\eta E + D^\eta A + D^\eta I \\ &= \frac{\beta S I}{1+\alpha I} - (\delta + d)E + k\delta E - (p+q+d)A + (1-k)\delta E + pA - (\nu + d + u)I \\ &\leq \frac{\beta \Lambda I}{d} - dE - (q+d)A - (\nu + d + u)I \\ &= -d(E+A) - \left(\nu + u + d - \frac{\beta\Lambda}{d}\right)I - qA. \end{aligned} \tag{3.12}$$

Thus, if $\nu + u + d - \frac{\beta\Lambda}{d} > 0$, then $D^\eta \mathcal{L}_1(S,E,A,I,R) < 0$, which implies that if $R_0 < 1$, the DFE P_0 is globally asymptotically stable. □

Theorem 3.7. *When $R_0 > \phi$, P^* is globally asymptotically stable within model (2.2) (see Figure 4).*

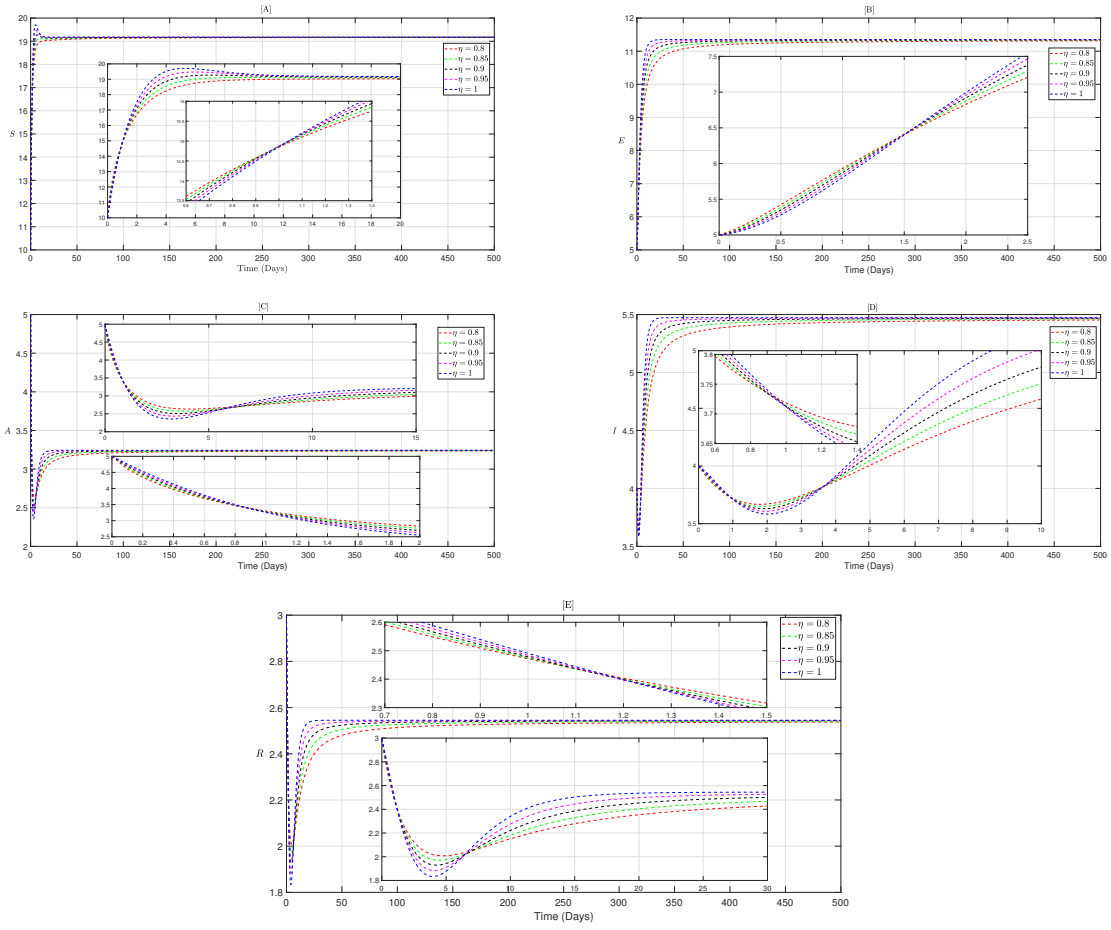

Figure 4. The dynamic behavior of model (2.2) when $R_0 > \phi$. Parameters: $\Lambda = 10, \beta = 0.2$, $\alpha = 0.3, d = 0.2, \sigma = 0.7, \delta = 0.5, k = 0.4, p = 0.3, q = 0.2, \nu = 0.3, u = 0.3$.

Proof. Define the Lyapunov function as

$$V_1(t) = S - S^*\left(1 + \ln\frac{S}{S^*}\right), \quad V_2(t) = E - E^*\left(1 + \ln\frac{E}{E^*}\right),$$

$$V_3(t) = A - A^*\Big(1 + \ln\frac{A}{A^*}\Big),\quad V_4(t) = I - I^*\Big(1 + \ln\frac{I}{I^*}\Big),\quad V_5(t) = R - R^*\Big(1 + \ln\frac{R}{R^*}\Big).$$

The calculation yields

$$\begin{aligned}
D^\eta V_1(t) &\le \left(1 - \frac{S^*}{S}\right)\left(\Lambda - dS - \frac{\beta S I}{1+\alpha I} + \sigma R\right)\\
&= dS^*\left(2 - \frac{S}{S^*} - \frac{S^*}{S}\right) + \frac{\beta S^* I^*}{1+\alpha I^*}\left(1 - \frac{S^*}{S} + \frac{1+\alpha I^*}{1+\alpha I}\Big(\frac{I}{I^*} - \frac{S I}{S^* I^*}\Big)\right) + \sigma R^*\left(1 + \frac{R}{R^*} - \frac{S^*}{S} - \frac{R S^*}{R^* S}\right),\\
D^\eta V_2(t) &\le \left(1 - \frac{E^*}{E}\right)\Big(\frac{\beta S I}{1+\alpha I} - dE - \delta E\Big) = \frac{\beta S^* I^*}{1+\alpha I^*}\left(1 - \frac{E}{E^*} + \frac{S I(1+\alpha I^*)}{S^* I^*(1+\alpha I)} - \frac{E^* S I(1+\alpha I^*)}{E S^* I^*(1+\alpha I)}\right),\\
D^\eta V_3(t) &\le \left(1 - \frac{A^*}{A}\right)(k\delta E - (p+q+d)A) = (p+q+d)\left(1 - \frac{A^*}{A} - \frac{E A^*}{E^* A} + \frac{E}{E^*}\right)A^*,\\
D^\eta V_4(t) &\le \left(1 - \frac{I^*}{I}\right)[(1-k)\delta E + pA - (u+\nu+d)I] = (u+\nu+d)\left(1 + \frac{1}{E^*} + \frac{A}{A^*} - \frac{I}{I^*} - \frac{I}{A^* I^*}\right)I^*,\\
D^\eta V_5(t) &\le \left(1 - \frac{R^*}{R}\right)[\nu I + qA - (d+\sigma)R] = \nu I^*\left(1 + \frac{I}{I^*} - \frac{R^* I}{R I^*} - \frac{R}{R^*}\right) + qA^*\left(1 + \frac{A}{A^*} - \frac{R}{R^*} - \frac{R^* A}{R A^*}\right).
\end{aligned} \tag{3.13}$$

By the arithmetic-geometric mean inequality [43], the solution is

$$\begin{aligned}
&2 - \frac{S}{S^*} - \frac{S^*}{S} \le 0,\quad 1 - \frac{S^*}{S} + \frac{1+\alpha I^*}{1+\alpha I}\Big(\frac{I}{I^*} - \frac{S I}{S^* I^*}\Big) \le 0,\quad 1 + \frac{R}{R^*} - \frac{S^*}{S} - \frac{R S^*}{R^* S} \le 0,\\
&1 - \frac{E}{E^*} - \frac{E^* S I(1+\alpha I^*)}{E S^* I^*(1+\alpha I)} + \frac{S I(1+\alpha I^*)}{S^* I^*(1+\alpha I)} \le 0,\quad 1 - \frac{A^*}{A} - \frac{E A^*}{E^* A} + \frac{E}{E^*} \le 0,\\
&1 + \frac{1}{E^*} + \frac{A}{A^*} - \frac{I}{I^*} - \frac{I}{A^* I^*} \le 0,\quad 1 + \frac{I}{I^*} - \frac{R^* I}{R I^*} - \frac{R}{R^*} \le 0,\quad 1 + \frac{A}{A^*} - \frac{R}{R^*} - \frac{R^* A}{R A^*} \le 0.
\end{aligned}$$

Then, we can obtain $D^\eta V \le D^\eta V_1 + D^\eta V_2 + D^\eta V_3 + D^\eta V_4 + D^\eta V_5 \le 0$. When $S = S^*, E = E^*, A = A^*, I = I^*, R = R^*$, $D_t^\eta V = 0$. By LaSalle's Invariance Principle [42], the equilibrium P^* is globally asymptotically stable. □

Remark 3.3. *Theorem 3.6 states that when $R_0 < 1$, the trajectories of model (2.2) will stabilize at the DFE P_0, regardless of the initial condition. In other words, without control measures, the flu will be naturally controlled. On the other hand, Theorem 3.7 indicates that when $R_0 > \phi$, the trajectories of model (2.2) will stabilize at the EE P^*, meaning that without control measures, the flu will spread.*

To further verify the correctness of the above theoretical results and to study the impact of η on the dynamical behavior of model (2.2), we use the FDE12 method to solve the fractional-order derivatives and visualize the results in Figures 3 and 4. As shown in the figures, when $R_0 < \phi$, model (2.2) stabilizes at the DFE P_0; when $R_0 > \phi$, it stabilizes at the EE P^*, further confirming the validity of the theoretical analysis. Additionally, it can be observed that as η increases, the system stabilizes more rapidly, which is attributed to the memory effect inherent in fractional-order models. The figures also indicate that the integer-order model is merely a special case of the fractional-order model, suggesting that the latter is more flexible and capable of adapting to more complex scenarios.

Moreover, to further analyze the impact of η and β on the dynamics of model (2.2), we fix the other parameters in model (2.2) and analyze the maximum values of each variable at the steady state of model (2.2) as η and β change, as shown in Figure 5. From the figure, we observe that as η increases, the number of susceptible individuals at the steady state of model (2.2) increases, while the numbers of the other four groups decrease. This is due to the fact that the steady state of the influenza model is influenced by past states. Additionally, we can see that the impact of β on the steady state of model (2.2) is the opposite of that of η, and when β is small, its impact on the steady state is also smaller. This further emphasizes that reducing the effective contact rate between symptomatic infected individuals and susceptible individuals is an important approach to controlling influenza.

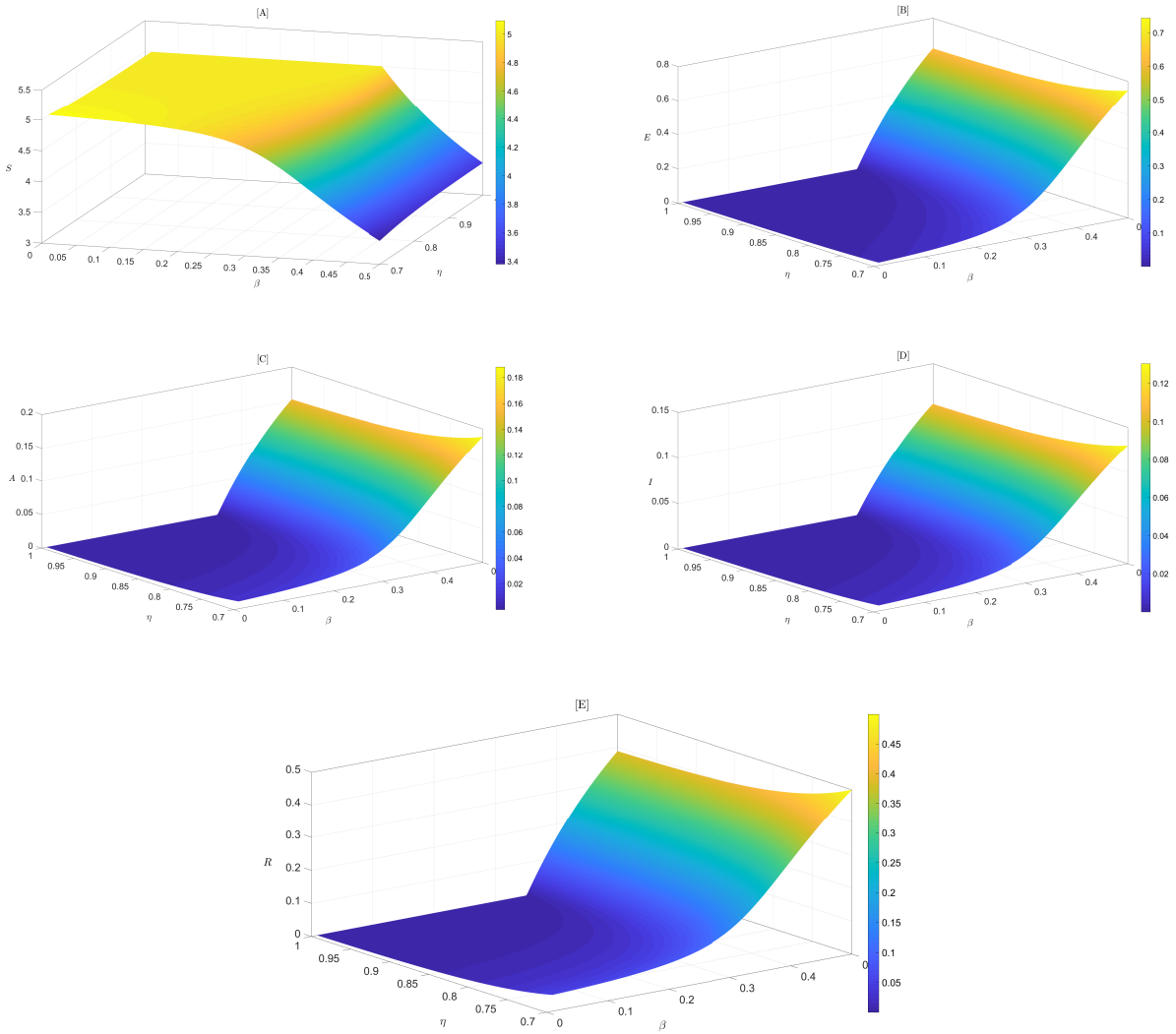

Figure 5. The maximum value of each variable in model (2.2) at a stable state as parameters β and η vary, with other parameters fixed at $d = 0.1$, $a = 0.01$, $\sigma = 0.1$, $k = 0.5$, $p = 0.01$, $q = 0.3$,$\Lambda = 0.5$, $\delta = 0.2$, $\nu = 0.3$, and $u = 0.2$.

3.5. Sensitivity analysis

Based on the above analysis, we can conclude that when $R_1 < 1$, the flu will subside, whereas when $R_1 > 1$, the flu will outbreak, with

$$R_1 = \frac{\beta\Lambda\delta\,(p+q+d-kq-kd)}{d\,(\delta+d)\,(p+q+d)\,(\nu+d+u)}.$$

Sensitivity analysis helps reveal the impact of model parameters on R_1 and flu transmission. Through this analysis, we can identify which parameters and initial conditions play a crucial role in the model's output and highlight the parameters that require more attention and precise computation [44, 45]. In the normalized forward sensitivity analysis, the sensitivity index of R_1 depends on the variation of parameter i, expressed as $\rho_i^{R_1} = \frac{\partial R_1}{\partial i} \times \frac{i}{R_1}$, where i represents any parameter in R_1. For example, the sensitivity index of R_1 with respect to parameter β is given by $\rho_\beta^{R_1} = \frac{\partial R_1}{\partial \beta} \times \frac{\beta}{R_1} = 1$. The sensitivity indices for other parameters are also calculated in a similar manner, with the results shown in Table 2. Additionally, the sensitivity indices of all parameters have been visualized, as shown in Figure 6.

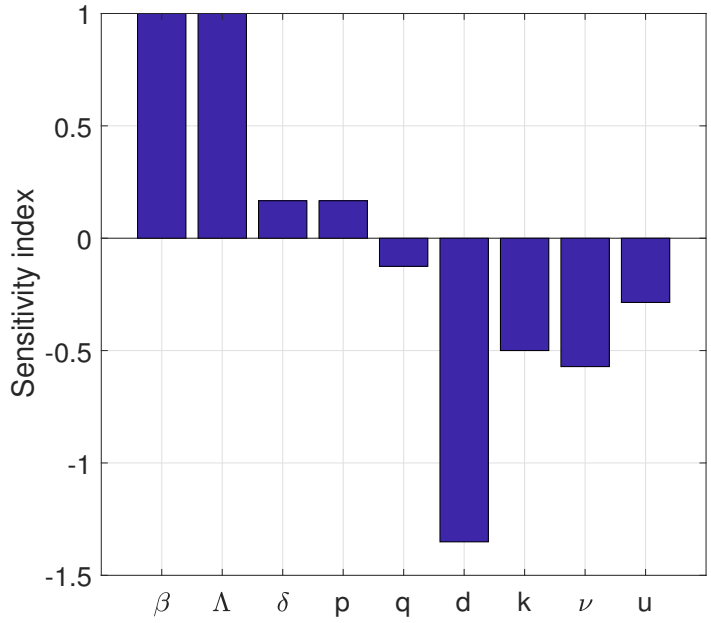

Figure 6. Sensitivity analysis plot of R_1 regarding the parameters of model (2.2).

Table 2. Calculate the parameter values of the R_1 sensitivity index and their corresponding sensitivity index values.

Parameter	Value	Sensitivity index	Parameter	Value	Sensitivity index
β	0.1	1	d	0.01	-1.3512
Λ	100	1	k	0.5	-0.5
δ	0.05	0.1667	ν	0.04	-0.5714
p	0.02	0.1667	u	0.02	-0.2857
q	0.03	-0.1250			

As shown in Figure 6, the continuous influx of population (Λ), the effective contact rate between symptomatic infected individuals and susceptible individuals (β), and the natural mortality rate of the population (d) have a significant impact on the spread of influenza. Among them, Λ and β promote the spread of influenza, while d acts to suppress it. Therefore, in controlling the spread of influenza, measures such as temporarily closing areas where influenza outbreaks occur, limiting the large-scale movement of the population to reduce the continuous influx of people, and implementing measures like wearing masks and home isolation to reduce the effective contact rate between symptomatic infected individuals and susceptible individuals can be effective. However, this does not imply that other parameters are unimportant for influenza transmission. For example, antiviral medications can be used to increase the rate at which symptomatic infected individuals transition to recovery (ν), which is also an important method for controlling the spread of influenza.

3.6. Bifurcation analysis

Bifurcation is an important dynamical behavior in influenza models. Bifurcation phenomena indicate that the dynamical behavior of model (2.2) can change significantly with small perturbations in one or more parameters. This sensitivity reflects the inherent complexity of influenza transmission. Moreover, by analyzing these bifurcation phenomena, we can gain a deeper understanding of influenza transmission mechanisms, while providing more precise control directions for influenza management. For example, if small perturbations in the effective contact rate β between susceptible and symptomatic infected individuals can lead to influenza outbreaks, then measures such as promoting mask-wearing in public or home isolation can be implemented to reduce or cut off the transmission of influenza.

Theorem 3.8. *Model (2.2) undergoes equilibrium bifurcation at $R_0 = \phi$.*

Proof. In Theorem 3.3, we have proved that model (2.2) has a DFE P_0, and if $R_0 > \phi$, there exists an EE P^*. That is, if $R_0 < \phi$, model (2.2) has only one equilibrium; when $R_0 > \phi$, there are two equilibria, therefore model (2.2) undergoes equilibrium bifurcation at $R_0 = \phi$. It is worth noting that when we fix other parameters and use any single parameter from $R_0 = \phi$ as the bifurcation parameter, a single-parameter equilibrium bifurcation will occur. For example, fixing other parameters and using Λ as the bifurcation parameter, model (2.2) undergoes equilibrium bifurcation at

$$\Lambda = \Lambda^* = \frac{d\,(\delta + d)\,(p + q + d)\,(\nu + d + u)}{\delta\beta\,(p + q + d - kq - kd)}.$$

Similarly, when fixing the remaining parameters and using multiple parameters from $R_0 = \phi$ as bifurcation parameters, model (2.2) will exhibit bifurcation phenomena. For instance, when using d and β simultaneously as bifurcation parameters, bifurcation occurs when d and β satisfy the equation $\beta = \frac{d(\delta+d)(p+q+d)(\nu+d+u)}{\delta\Lambda(p+q+d-kq-kd)}$, as shown in Figure 7A; likewise, when using β and Λ as bifurcation parameters, bifurcation occurs when β and Λ satisfy

$$\beta\Lambda = \frac{d\,(\delta + d)\,(p + q + d)\,(\nu + d + u)}{\delta\,(p + q + d - kq - kd)},$$

as shown in Figure 7B. □

Theorem 3.9. *Model (2.2) undergoes a transcritical bifurcation near the DFE P_0 when $R_0 = \phi$.*

Proof. According to Theorem 1, if $R_0 < \phi$, model (2.2) has only one DFE; if $R_0 > \phi$, there exists one DFE and one EE. Moreover, Theorems 2 and 3 indicate that when $R_0 < \phi$, the DFE of model (2.2) is locally asymptotically stable; when $R_0 > \phi$, the EE of model (2.2) is globally stable. That is, near $R_0 = \phi$, the stability of model (2.2) changes. Based on reference [46], we can infer that model (2.2) undergoes a transcritical bifurcation at $R_0 = \phi$, as shown in Figure 8B. Now, keeping other parameters fixed and using only β as the bifurcation parameter, model (2.2) undergoes a transcritical bifurcation at $\beta = \frac{d(\delta+d)(p+q+d)(\nu+d+u)}{\delta\Lambda(p+q+d-kq-kd)}$, as shown in Figure 8A. By substituting the specific values of the fixed parameters from Figure 8 into $R_0 = \phi$, we can determine that model (2.2) undergoes a transcritical bifurcation at $R_0 = 3.75$ and $\beta = 0.45$. □

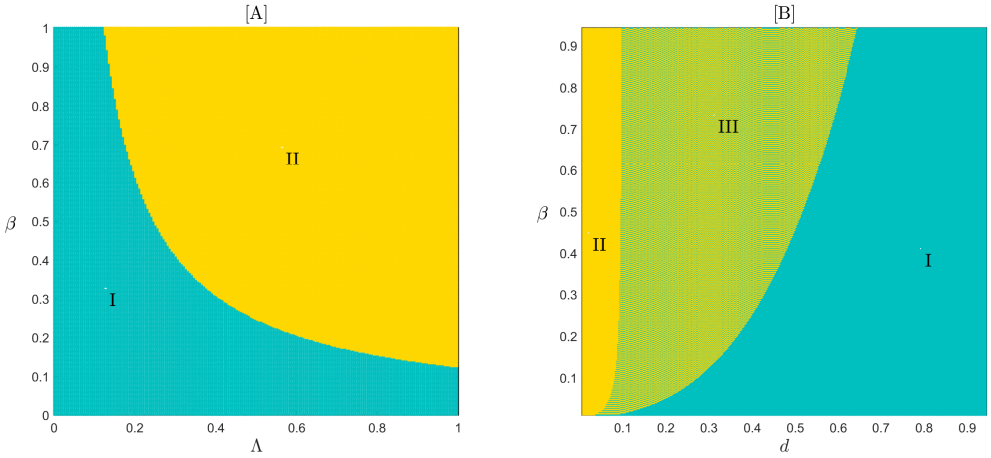

Figure 7. The bifurcation of model (2.2), where Region I represents only one DFE, Region II represents one DFE and one EE, and Region III represents sensitivity to bifurcation parameters, where slight perturbations can change the number of equilibria. Parameters: [A] $\alpha = 0.5$, $\sigma = 0.2$, $\delta = 0.3$, $k = 0.7$, $p = 0.2$, $q = 0.1$, $\nu = 0.2$, $u = 0.3$, $d = 0.1$. [B] $\alpha = 0.5$, $\sigma = 0.2$, $\delta = 0.5$, $k = 0.8$, $p = 0.2$, $q = 0.1$, $\nu = 0.2$, $u = 0.1$, and $\Lambda = 7$.

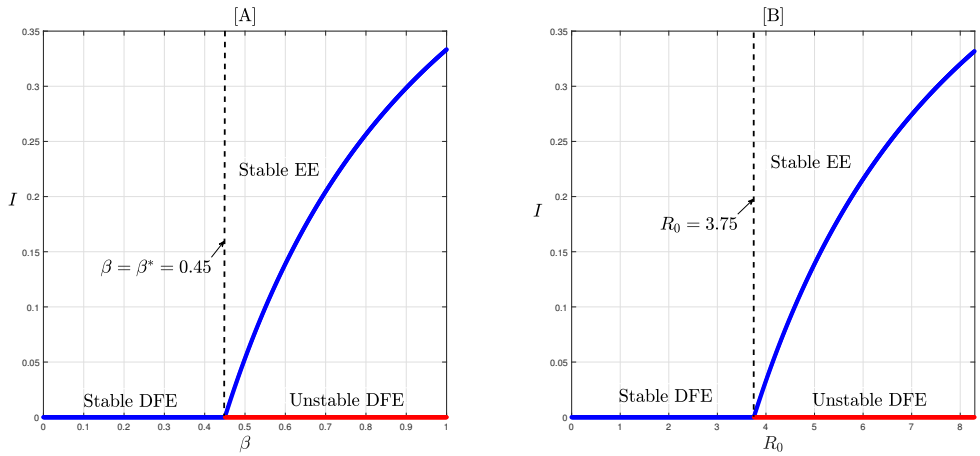

Figure 8. The transcritical bifurcation of model (2.2) with the bifurcation parameter β, and the other parameters fixed as $\Lambda = 2$, $\alpha = 0.5$, $d = 0.3$, $\sigma = 0.2$, $\delta = 0.3$, $k = 0.7$, $p = 0.2$, $q = 0.1$, $\nu = 0.2$, and $u = 0.3$.

Remark 3.4. *From Figures 7 and 8, we can see that when the effective contact rate (β) between symptomatic infecteds and susceptibles is low, influenza does not outbreak. However, when β is large enough, such that $R_0 > \phi$, an outbreak will occur, and the outbreak severity increases as β increases. The impact of the constant input of susceptible individuals (Λ) on the influenza dynamics is similar to that of β, while the natural death rate of the population (d) has the opposite effect.*

4. Fractional optimal control

Early isolation or vaccination strategies play a crucial role in controlling the spread of influenza. In this context, we incorporate these control strategies into the model. Specifically, early vaccination and isolation help reduce the number of exposed individuals and assist in converting asymptomatic infecteds into recoveries. To capture the effect of these control strategies, we introduce a control function $c(t) \in [0, 1]$. However, due to the limited isolation spaces and medical resources, when multiple exposed individuals are confined in the same space, some of them may convert into symptomatic infecteds. Based on this, model (2.2) can be modified as

$$\begin{aligned}
&{}^{C}D_t^{\eta} S(t) = \Lambda - \tfrac{\beta S I}{1+\alpha I} - dS + \sigma R,\\
&{}^{C}D_t^{\eta} E(t) = \tfrac{\beta S I}{1+\alpha I} - (\delta + c + d)E,\\
&{}^{C}D_t^{\eta} A(t) = k\delta E - (p + q + c + d)A,\\
&{}^{C}D_t^{\eta} I(t) = (1 + c - k)\delta E + pA - (\nu + d + u)I,\\
&{}^{C}D_t^{\eta} R(t) = (q + c)A + \nu I - (\sigma + d)R.
\end{aligned} \tag{4.1}$$

To obtain the optimal solution of model (2.2), define the objective function

$$O(c) = \min_c \int_0^T L(E(t), A(t), I(t), c(t)) = \min_c \int_0^T \Big(w_1 E(t) + w_2 A(t) + w_3 I(t) + \frac{w_4}{2} c(t)^2\Big) dt, \tag{4.2}$$

where w_1, w_2, w_3, and w_4 are positive weights associated with exposed individuals, asymptomatic infected individuals, symptomatic infected individuals, and the treatment control parameter $c(t)$, respectively. w_1 represents the cost impact of exposed individuals, w_2 and w_3 represent the cost contributions of asymptomatic and symptomatic infected individuals, and w_4 reflects the impact of treatment control on the cost. The control level $c(t)$ ranges within $[0, 1]$, it reaches $c(t) = 1$ under severe outbreak conditions and drops to $c(t) = 0$ when no infection is present.

4.1. The presence of optimal control

Let Φ be the control set, and there exists a $c^* \in \Phi$ such that the $O(c)$ is minimized, i.e.,

$$O(c^*) = \min_{c \in \Phi} O(c). \tag{4.3}$$

Theorem 4.1. *If these conditions are all fulfilled:*
(i) Φ and its associated state variables form a non-empty set;
(ii) Φ is both closed and convex;
(iii) The right-hand side of model (4.1) exhibits linearity in terms of the state and control set;

(iv) The integral and $L(E, A, I, c)$ is convex on Φ;
(v) There are defined positive constants k_1 and k_2, along with $\beta > 1$, for which $L(E, A, I, c)$ satisfies

$$L(E, A, I, c) \geq k_1|c|^{\beta} - k_2, \tag{4.4}$$

then there exists $c^* \in \Phi$ such that $O(c^*) = \min_{c\in\Phi} O(c)$.

Proof. Based on the existence of bounded system solutions and the definition of the control set [47], conditions (i) and (ii) hold. We focus on proving the last three conditions, and below is the proof for condition (iii):

First, we simplify model to obtain $D^{\eta}X(t) = M(X) = NX(t) + O(X)$, where

$$X(t) = (S(t), E(t), A(t), I(t), R(t))^T,$$

$$N = \begin{pmatrix} -d & 0 & 0 & 0 & 0 \\ 0 & \delta + c + d & 0 & 0 & 0 \\ 0 & 0 & p + q + d & 0 & 0 \\ 0 & 0 & 0 & -(\nu + \alpha + u) & 0 \\ 0 & 0 & 0 & 0 & -(\sigma + d) \end{pmatrix}, \quad O(X) = \begin{pmatrix} \Lambda - \frac{\beta S I}{1+\alpha I} + \sigma R \\ \frac{\beta S I}{1+\alpha I} \\ k\delta E \\ (1 + c - k)\delta E + pA \\ (q + c)A + \nu I \end{pmatrix}.$$

Obviously, there exists a constant e^*, for which

$$S(t), E(t), A(t), I(t), R(t) < e^*.$$

Let $X_1(t) = (S_1(t), E_1(t), A_1(t), I_1(t), R_1(t))$ and $X_2(t) = (S_2(t), E_2(t), A_2(t), I_2(t), R_2(t))$. Thus, the Holder inequality [48], yields

$$\begin{aligned} |O(X_1) - O(X_2)| = 2\frac{\beta}{\alpha}\left|\frac{S_2 I_2}{\frac{1}{\alpha} + I_2} - \frac{S_1 I_1}{1 + I_1}\right| + \sigma|R_1 - R_2| + (1 + c)\delta|E_1 - E_2| \\ + (p + q + c)|A_1 - A_2| + \nu|I_1 - I_2|. \end{aligned}$$

Therefore,

$$\begin{aligned} |O(X_1) - O(X_2)| &\leq 2\frac{\beta}{\alpha}|I_1 I_2||S_1 - S_2| + 2\frac{\beta}{\alpha^2}|I_1||S_1 - S_2| + 2\frac{\beta}{\alpha^2}|S_2||I_1 - I_2| + \sigma|R_1 - R_2| \\ &\quad + (1 + c)\delta|E_1 - E_2| + (p + q + c)|A_1 - A_2| + \nu|I_1 - I_2| \\ &= \left(2\frac{\beta}{\alpha}|I_1 I_2| + 2\frac{\beta}{\alpha^2}|I_1|\right)|S_1 - S_2| + \left(2\frac{\beta}{\alpha^2}|S_2| + \nu\right)|I_1 - I_2| + \sigma|R_1 - R_2| \\ &\quad + (1 + c)\delta|E_1 - E_2| + (p + q + c)|A_1 - A_2| \\ &\leq \theta(|S_1 - S_2| + |I_1 - I_2| + |E_1 - E_2| + |A_1 - A_2| + |R_1 - R_2|), \end{aligned}$$

where

$$\theta = \max\left\{2\frac{\beta}{\alpha}(e^*)^2 + 2\frac{\beta}{\alpha^2}e^*, 2\frac{\beta}{\alpha^2}e^* + \nu, (1 + c)\delta, p + q + c\right\}.$$

This implies $|M(X_1) - M(X_2)| \leq \gamma|X_1 - X_2|$, where $\gamma = \max\{\theta, ||N||\} < \infty$. Thus, the function M is Lipschitz continuous. This implies that condition (iii) is satisfied.

Next, we demonstrate condition (iv). Let

$$L(t,E,A,I,c) = w_1E + w_2A + w_3I + \frac{w_4}{2}c^2,$$

where $c, m \in \Omega$ and $0 \le n \le 1$. To prove that L is convex, it suffices to demonstrate that

$$(1-n)L(t,E,A,I,c) + nL(t,E,A,I,m) \ge L(t,E,A,I,(1-n)c + nm),$$

namely

$$\begin{aligned}
&(1-n)L(t,E,A,I,c) + nL(t,E,A,I,m) - L(t,E,A,I,(1-n)c + nm)\\
&= (1-n)\left[w_1E + w_2A + w_3I + \frac{w_4}{2}c^2\right] + n\left[w_1E + w_2A + w_3I + \frac{w_4}{2}c^2\right]\\
&- \left[w_1E + w_2A + w_3I + \frac{w_4}{2}((1-n)c)^2\right]\\
&= \frac{w_4}{2}c^2 - n\frac{w_4}{2}c^2 + n\frac{w_4}{2}m^2 - \frac{w_4}{2}((1-n)c + nm)^2\\
&= \frac{w_4}{2}(1-n)n(c-m)^2 \ge 0.
\end{aligned}$$

This forms a convex function over Ω.

As $L(t,E,A,I,c)$ is a convex function. Thus,

$$w_1E + w_2A + w_3I + \frac{w_4}{2}c^2 \ge k_1|c|^n - k_2.$$

In this case, by choosing $k_1 = \frac{w_4}{2}$, any $k_2 > 0$ and $n = 2$, condition (v) is satisfied. □

4.2. Optimal system

According to Theorem 4.1, model (4.1) has an optimal solution. To determine the explicit expression for the optimal solution $c^*(t)$, we define the associated Lagrangian L and Hamiltonian H as

$$\begin{aligned}
L(E,I,c) &= w_1E + w_2A + w_3I + \frac{w_4}{2}c^2,\\
H(S,E,A,I,R,c,\lambda_1,\lambda_2,\lambda_3,\lambda_4,\lambda_5)&\\
= L(E,I,c) + \lambda_1D^\eta S + \lambda_2D^\eta E + \lambda_4D^\eta + \lambda_3D^\eta I + \lambda_4D^\eta R,&
\end{aligned}$$

where $\lambda_i(t)(i = 1,2,3,4,5)$ is the adjoint variable. By further applying the Pontryagin maximum principle [49, 50], the following state equation can be derived

$$\begin{aligned}
D^\eta\lambda_1(t) &= -\frac{\partial H}{\partial S} = \lambda_1(t)\left(d + \frac{\beta I}{1+\alpha I}\right) - \lambda_2(t)\frac{\beta I}{1+\alpha I},\\
D^\eta\lambda_2(t) &= -\frac{\partial H}{\partial E} = -w_1 + \lambda_2(t)(d+c+\delta) - \lambda_3(t)k\delta - \lambda_4(t)(1+c-k)\delta,\\
D^\eta\lambda_3(t) &= -\frac{\partial H}{\partial A} = -w_2 + \lambda_3(t)(d+p+q+c) - \lambda_4(t)p - \lambda_5(t)(q+c),\\
D^\eta\lambda_4(t) &= -\frac{\partial H}{\partial I} = -w_3 + \lambda_1(t)\frac{\beta S}{(1+\alpha I)^2} - \lambda_2(t)\frac{\beta S}{(1+\alpha I)^2} + \lambda_4(t)(\nu + d + u) - \lambda_5(t)\nu,\\
D^\eta\lambda_5(t) &= -\frac{\partial H}{\partial R} = -\lambda_1(t)\sigma + \lambda_5(t)(d+\sigma),
\end{aligned} \tag{4.5}$$

simultaneously satisfying the transversality condition $\lambda_1(T) = \lambda_2(T) = \lambda_3(T) = \lambda_4(T) = \lambda_5(T) = 0$. Let $\bar{S}$, $\bar{E}$, $\bar{A}$, $\bar{I}$, $\bar{R}$ represent the optimal solutions and $\bar{\lambda_1}, \bar{\lambda_2}, \bar{\lambda_3}, \bar{\lambda_4}, \bar{\lambda_5}$ be the solutions of the adjoint model (4.5). Based on the principles of optimal control, we derive the Theorem 4.2.

Theorem 4.2. *Let c^* denote the optimal control parameter. Within the λ range that minimizes O, c^* is expressed as follows*

$$c^* = max\left\{0, min\left\{\frac{\left(\bar{\lambda_2} - \bar{\lambda_4}\delta\right)\bar{E} + \bar{\lambda_3}\bar{A}}{w_3}, 1\right\}\right\}.$$

Proof. According to the necessary conditions of the control equation, $\frac{\partial H}{\partial c} = 0$, we obtain $c^* = \frac{(\bar{\lambda_2} - \bar{\lambda_4}\delta)\bar{E} + \bar{\lambda_3}\bar{A}}{w_3}$. From the preceding discussion, it follows that $0 < c < 1$. Consequently, if $c^* < 0$, then $c = 0$; if $c^* > 1$, then $c = 1$; otherwise $c = c^*$. Thus, the ideal range for c is 0 to

$$c^* = max\left\{0, min\left\{\frac{\left(\bar{\lambda_2} - \bar{\lambda_4}\delta\right)\bar{E} + \bar{\lambda_3}\bar{A}}{w_3}, 1\right\}\right\}.$$

□

To comprehensively study the impact of initial infection levels and the parameter η on influenza control strategies, we conduct a numerical simulation analysis within the framework of optimal control theory. Figures 9A, 10, and 11 illustrate the temporal evolution of the model's state variables and the objective function O under different initial infection levels, with initial state vectors given as $X_{01} = [100, 50, 40, 30, 20]$, $X_{02} = [200, 80, 60, 40, 30]$, $X_{03} = [400, 200, 150, 100, 80]$, and $X_{04} = [600, 300, 200, 150, 80]$. In contrast, Figures 9B, 12, and 13 show the model's dynamic response to changes in the parameter η, with parameter values set to $\eta_1 = 0.7$, $\eta_2 = 0.8$, $\eta_3 = 0.9$, and $\eta_4 = 1$.

In Figures 9A, 10, and 11, regardless of the initial numbers of exposed individuals, symptomatic infectives, and asymptomatic carriers, as long as the control strategy is appropriate, the optimal control trajectory $c(t)$ undergoes intense intervention in the early phase and gradually converges to a common steady state. Furthermore, the objective function O rapidly decays and tends toward equilibrium. This suggests that, in the actual control of influenza, government departments should invest sufficient manpower and resources in the early stages of intervention. For example, early efforts can include encouraging the public to purchase influenza antiviral drugs, get vaccinated, wear qualified masks, and implement isolation measures. As the flu transmission situation changes, the intensity of control measures can be adjusted appropriately to ensure that resources are not wasted while effectively controlling the spread of influenza.

In contrast, Figures 9B, 12, and 13 indicate that as the value of η increases, a longer maximum control duration and higher costs are required for influenza control. This reflects the complexity and diversity of flu transmission. Influenza in different times and regions may require different orders of flu models (represented by η) for prediction. The appropriate value of η can effectively predict the transmission trend of influenza over a given period, thus helping to develop reasonable control strategies. However, when the value of η is chosen incorrectly, it may lead to excessive or insufficient control investments, wasting resources and potentially resulting in the failure of influenza control.

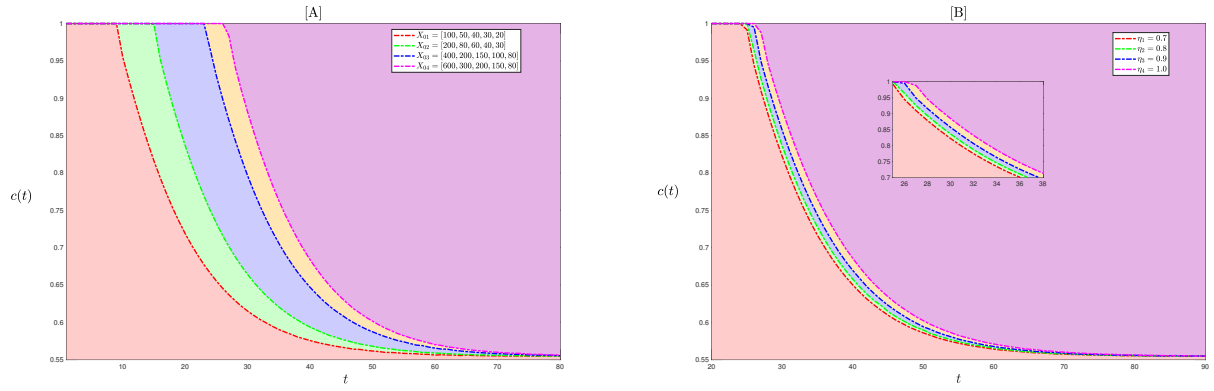

Figure 9. The time series of the control parameter $c(t)$ under different initial values and parameters. [A] represents the time series for different initial values X_{0i} $(i = 1, 2, 3, 4)$ and [B] represents the time series for different parameters η_i $(i = 1, 2, 3, 4)$. The fixed parameter set is $\Lambda = 3.4, \beta = 0.3, \alpha = 1.56, d = 0.02, \sigma = 0.45, \delta = 0.35, k = 0.7, p = 0.25, q = 0.5, \nu = 0.3, u = 0.2$, and $\eta = 0.99$.

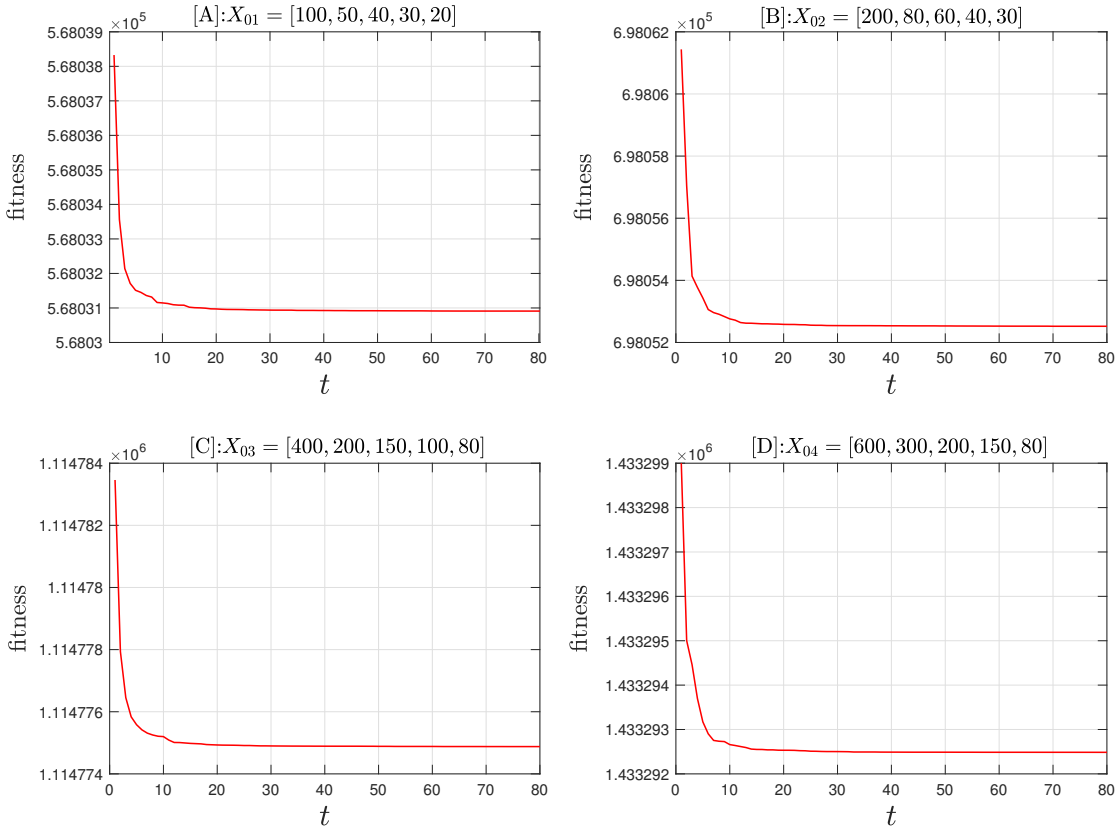

Figure 10. The time series of the objective function O under different initial values.The parameter set is the same as in Figure 9.

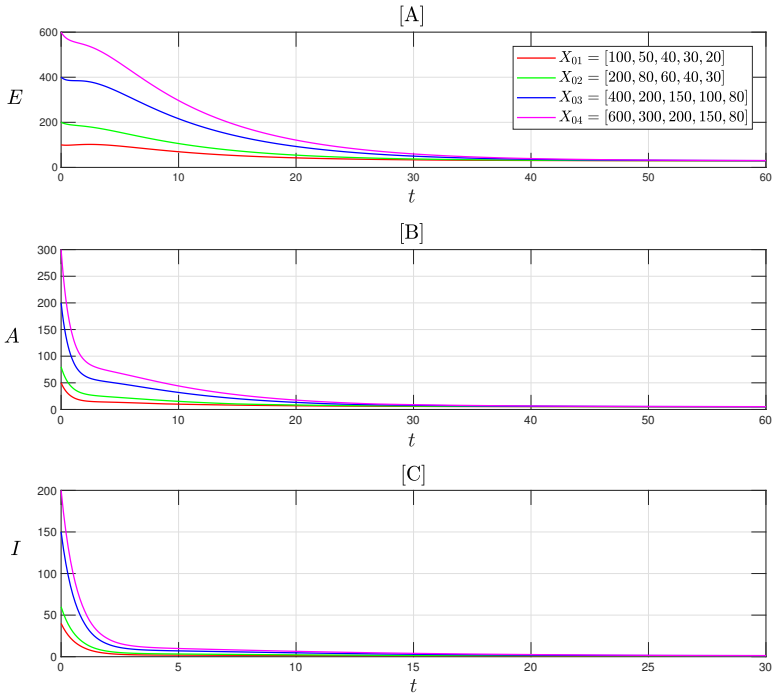

Figure 11. Dynamic behavior of the model (2.2) under different initial values. The parameter set is the same as in Figure 9.

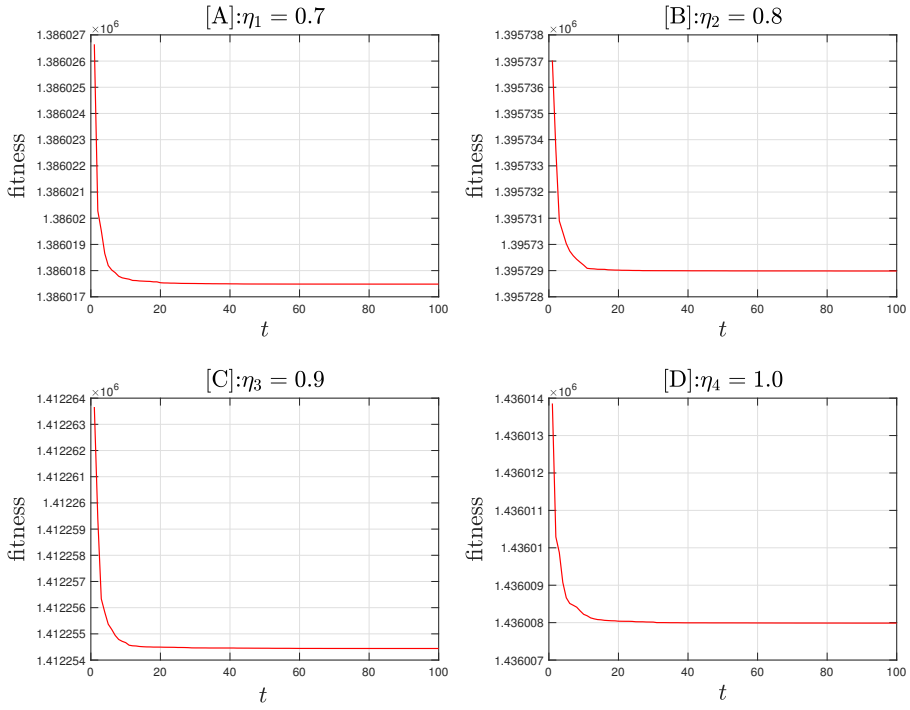

Figure 12. The time series of the objective function O under different values of η. The parameter set is the same as in Figure 9.

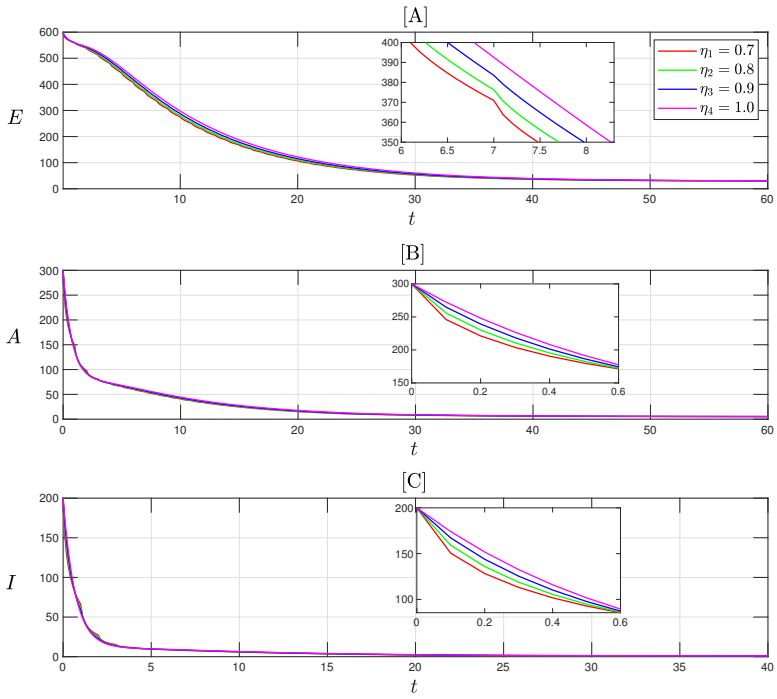

Figure 13. The dynamic behavior of model (2.2) at different η. The parameter set is the same as in Figure 9.

5. Stochastic stability of model (2.2) at P^* with $\eta = 1$

The transmission of influenza exhibits significant randomness, typically influenced by factors such as the environment, policy changes, and resource availability. In modeling, stochastic models are usually constructed by introducing small perturbations around the steady-state solution of the deterministic model, combined with white noise. This white noise can be classified into two types: One type perturbs one or more key parameters with white noise; the other type perturbs all model parameters [51]. In this paper, we adopt the second type of model, aiming to investigate the fluctuation effects of the entire system. Specifically, small perturbations will be introduced around the epidemic equilibrium $P^* = (S^*, E^*, A^*, I^*, R^*)$, with these perturbations being proportional to the deviations in $S(t)$, $E(t)$, $I(t)$, and $R(t)$, corresponding to the deviations from S^*, E^*, A^*, I^*, and R^*, respectively. In this section, we consider only the special case where $\eta = 1$. Therefore, model (2.2) can be modified as follows:

$$\begin{cases} dS = \left[\Lambda - \frac{\beta S I}{1+\alpha I} - dS + \sigma R\right]dt + \mu_1(S - S^*)d\zeta_1, \\ dE = \left[\frac{\beta S I}{1+\alpha I} - (\delta + d)E\right]dt + \mu_2(E - E^*)d\zeta_2, \\ dA = \left[k\delta E - (p + q + d)A\right]dt + \mu_3(A - A^*)d\zeta_3, \\ dI = \left[(1 - k)\delta E + pA - (\nu + d + u)I\right]dt + \mu_4(I - I^*)d\zeta_4, \\ dR = \left[qA + \nu I - (\sigma + d)R\right]dt + \mu_5(R - R^*)d\zeta_5. \end{cases} \tag{5.1}$$

Here, μ_i $(i = 1, 2, 3, 4)$ represents the non-negative intensities of environmental fluctuations. Specifically, μ_1 denotes the perturbation intensity when S (susceptible individuals) deviates from its equilibrium value S^*, which is closely related to external random factors such as environmental changes, adjustments in public health policies, and resource allocation; μ_2 represents the perturbation intensity when E (exposed individuals) deviates from E^*, reflecting the impact of transmission rate fluctuations, changes in exposure pathways, and other factors on the system; μ_3 represents the perturbation intensity related to asymptomatic carriers, such as undetected sources of infection, activities of latent infections, or inadequate health monitoring; μ_4 denotes the perturbation intensity when I (infected individuals) deviates from its equilibrium value I^*, which is related to the disease transmission rate, the effectiveness of treatment measures, isolation effects, and changes in public health policies; μ_5 describes the perturbation intensity when R (recovered individuals) deviates from R^*, influenced by factors such as individual immune responses, fluctuations in vaccination rates, and variations in treatment efficacy. $\zeta(t) = (\zeta_1(t), \ldots, \zeta_5(t))$ represents a five-dimensional standard Brownian motion, modeling a white noise process. Both models have the same equilibrium P^*, and when $\mu_i = 0$ $(i = 1, 2, 3, 4)$, model (2.2) degenerates into model (5.1). The above stochastic model (5.1) can be expressed in the form of an Ito differential equation system as

$$dX(t) = f(X(t))dt + g(X(t))d\zeta(t), X(t_0) = X_0, t\in[t_0, T],$$

where $X(t)$ represents the solution set of model (5.1), $d\zeta = (d\zeta_1, d\zeta_2, d\zeta_3, d\zeta_4, d\zeta_5)^T$. Additionally, we introduce four new variables: $z_1 = S - S^*$, $z_2 = E - E^*$, $z_3 = A - A^*$, $z_4 = I - I^*$, and $z_5 = R - R^*$. Linearizing around P^* yields

$$dz(t) = f(z(t))dt + g(z(t))d\zeta, \tag{5.2}$$

where $z(t) = (z_1(t), z_2(t), z_3(t), z_4(t), z_5(t))^T$.

$$f(z(t)) = \begin{bmatrix} -c_1 z_1 & 0 & 0 & -c_2 z_4 & \sigma z_5 \\ c_3 z_1 & -c_4 z_2 & 0 & c_2 z_4 & 0 \\ 0 & k\delta z_2 & -c_5 z_3 & 0 & 0 \\ 0 & (1-k)\delta z_2 & p z_3 & -c_6 z_4 & 0 \\ 0 & 0 & q z_3 & \nu z_4 & -c_7 z_5 \end{bmatrix},$$

$$g(z(t)) = \begin{bmatrix} \mu_1 z_1 & 0 & 0 & 0 & 0 \\ 0 & \mu_2 z_2 & 0 & 0 & 0 \\ 0 & 0 & \mu_3 z_3 & 0 & 0 \\ 0 & 0 & 0 & \mu_4 z_4 & 0 \\ 0 & 0 & 0 & 0 & \mu_5 z_5 \end{bmatrix},$$

$$c_1 = \frac{\beta I}{1+\alpha I} + d, c_2 = \frac{\beta S}{(1+\alpha I)^2}, c_3 = \frac{\beta S}{1+\alpha I},$$

$$c_4 = \delta + d, c_5 = p + q + d, c_6 = \nu + d + u, c_7 = \sigma + d.$$

Clearly, model (5.1) has the same internal equilibrium as model (2.2), i.e., $z(t) = 0$.

Next, we analyze the situation where $U \in C_2(\Theta)$, where Θ is the space of all $(t, \mathbb{R}^4)$ combinations and $t_0 \in \mathbb{R}^+$. The function U is continuously differentiable of order two with respect to the z-direction. In this case, Lemma 5.1 is invoked.

Lemma 5.1 ([52]). *Assume $U(z,t) \in C_2(\Theta)$ to comply with the following inequalities*

$$K_1|z|^p \leq U(z,t) \leq K_2|z|^p, \tag{5.3}$$

$$LU(z,t) \leq -K_3|z|^p, K_i > 0(i = 1,2,3), P > 0. \tag{5.4}$$

Thus, model (5.2) demonstrates exponential p-stability beyond $t = 0$.

We introduce the operator L, i.e.,

$$LU(z(t),t) = U_t(z(t),t) + f^T(z(t))U_z(z(t),t) + \frac{1}{2}\text{trace}\Big[g^T(z(t),t)U_{zz}(z(t),t)g(z(t),t)\Big],$$

where

$$U_z(z(t),t) = col\Big(\frac{\partial U}{\partial z_1}, \frac{\partial U}{\partial z_2}, \frac{\partial U}{\partial z_3}, \frac{\partial U}{\partial z_4}, \frac{\partial U}{\partial z_5}\Big), U_{zz}(z(t),t) = \Big(\frac{\partial^2 U}{\partial z_i \partial z_j}\Big), i, j = 1,2,3,4,5.$$

By setting $p = 2$ in Eqs (5.3) and (5.4), we establish that the trivial solution of (5.2) achieves global asymptotic stability in probability.

Theorem 5.1. *The trivial solution of model (5.1) is asymptotically stable in the mean square sense when*

$$\mu_1^2 < 2\Big(c_1 - A^2 - B^2\Big),\ \mu_2^2 < 2\Big(-D^2 - E^2 - c_4\Big),$$

$$\mu_3^2 < 2\Big(c_5 - \frac{1}{2} - F^2 - G^2 - q\Big),\ \mu_4^2 < 2\Big(\nu - c_6 - H^2 - \frac{1}{2}\Big),\ \mu_5^2 < 2\Big(d - 3c_7 - I^2\Big),$$

where A, B, D, E, and F are subsequently determined.

Proof. We utilize the following Lyapunov function [30]

$$U(z,t) = U_1(z,t) + U_2(z,t) + U_3(z,t) + U_4(z,t), \tag{5.5}$$

where

$$U_1(z,t) = \frac{1}{2}\left(z_1^2 + z_5^2\right), U_2(z,t) = \frac{1}{2}\left(z_2^2 + z_5^2\right), U_4(z,t) = \frac{1}{2}\left(z_3^2 + z_5^2\right), U_3(z,t) = \frac{1}{2}\left(z_4^2 + z_5^2\right).$$

It is straight forward to verify that inequality (5.3) holds when $p = 2$.

By applying the operator L, we obtain

$$\begin{aligned} LU_1 = &-\left(c_1 - \frac{1}{2}\mu_1^2\right)z_1^2 - \left(d - \frac{1}{2}\mu_5^2\right)z_5^2 + qz_1z_3 + (\nu - c_2)z_1z_4 \\ &- (d + c_1)z_1z_5 + qz_3z_5 + (\nu - c_2)z_4z_5. \end{aligned} \tag{5.6}$$

Similarly, we have

$$\begin{aligned} LU_2 = &\left(-c_4 + \frac{1}{2}\mu_2^2\right)z_2^2 + \left(-c_7 + \frac{1}{2}\mu_5^2\right)z_5^2 + qz_3z_4 + (c_2 + \nu)z_2z_4 \\ &- c_7z_2z_5 - c_3z_1z_5 - c_4z_2z_5 + qz_3z_5 + (c_2 + \nu)z_4z_5, \end{aligned} \tag{5.7}$$

$$\begin{aligned} LU_3 =& \left(q - c_5 + \frac{1}{2}\mu_3^2\right) z_3^2 + \left(-c_7 + \frac{1}{2}\mu_5^2\right) z_5^2 + k\delta z_2 z_3 + \nu z_3 z_4 \\ &+ k\delta z_2 z_5 + (q - c_5 - c_7) z_3 z_5 + \nu z_4 z_5, \end{aligned} \tag{5.8}$$

$$\begin{aligned} LU_4 =& \left(\nu - c_6 + \frac{1}{2}\mu_4^2\right) z_4^2 + \left(-c_7 + \frac{1}{2}\mu_5^2\right) z_5^2 + (1-k)\delta z_2 z_4 + (p+q) z_3 z_4 \\ &+ (1-k)\delta z_2 z_5 + (q+p) z_3 z_5 + (\nu - c_6 - c_7) z_4 z_5. \end{aligned} \tag{5.9}$$

Now, utilizing Eqs (5.6), (5.7), and (5.9) in (5.5) and simplifying, we obtain

$$\begin{aligned} \mathrm{LU} =& -\left(c_1 - \frac{1}{2}\mu_1^2\right) z_1^2 - \left(-c_4 + \frac{1}{2}\mu_2^2\right) z_2^2 - \left(-q + c_5 - \frac{1}{2}\mu_3^2\right) z_3^2 \left(\nu - c_6 + \frac{1}{2}\mu_4^2\right) z_4^2 \\ &- \left(d - 3c_7 + 2\mu_5^2\right) z_5^2 + A z_1 z_3 + B z_1 z_4 + C z_1 z_5 + D z_2 z_3 + E z_2 z_4 + F z_2 z_5 \\ &+ G z_3 z_4 + H z_3 z_5 + I z_4 z_5, \end{aligned} \tag{5.10}$$

where

$$\begin{aligned} &A = q, B = \nu - c_2 - d - c_1, C = -c_3 < 0, D = k\delta, \\ &E = c_2 + \nu + (1-k)\delta, F = \delta - c_4 - c_7, G = 2q + p + \nu, \\ &H = 4q + p - c_5 - c_7, I = 4\nu - c_6 - c_7. \end{aligned}$$

Utilizing the relationship between arithmetic and geometric means, we have

$$\begin{aligned} &A z_1 z_3 \le A^2 z_1^2 + \frac{z_3^2}{4}, B z_1 z_4 \le B^2 z_1^2 + \frac{z_4^2}{4}, D z_2 z_3 \le D^2 z_2^2 + \frac{z_3^2}{4}, E z_2 z_4 \le E^2 z_2^2 + \frac{z_4^2}{4}, \\ &F z_3 z_4 \le F^2 z_3^2 + \frac{z_4^2}{4}, G z_3 z_4 \le G^2 z_3^2 + \frac{z_4^2}{4}, H z_3 z_5 \le H^2 z_3^2 + \frac{z_4^5}{4}, I z_4 z_5 \le I^2 z_4^2 + \frac{z_4^5}{4}. \end{aligned}$$

Applying these relationships transforms (5.10) into

$$\begin{aligned} LU \le& -\left(c_1 - A^2 - B^2 - \frac{1}{2}\mu_1^2\right) z_1^2 - \left(\frac{1}{2}\mu_2^2 - D^2 - E^2 - c_4\right) z_2^2 \\ &- \left(c_5 - \frac{1}{2} - F^2 - G^2 - q - \frac{1}{2}\mu_3^2\right) z_3^2 - \left(\nu - c_6 - H^2 - \frac{1}{2} + \frac{1}{2}\mu_4^2\right) z_4^2 \\ &- \left(d - 3c_7 + 2\mu_5^2 - I^2 - \frac{1}{2}\right) z_5^2. \end{aligned} \tag{5.11}$$

If $\mu_1^2 < 2(c_1 - A^2 - B^2)$, $\mu_2^2 < 2(-D^2 - E^2 - c_4)$, $\mu_3^2 < 2\left(c_5 - \frac{1}{2} - F^2 - G^2 - q\right)$, $\mu_4^2 < 2\left(\nu - c_6 - H^2 - \frac{1}{2}\right)$ and $\mu_5^2 < 2(d - 3c_7 - I^2)$, then from the above equations, we can express

$$LU \le -\left(P_1 z_1^2 + P_2 z_2^2 + P_3 z_3^2 + P_4 z_4^2 + P_5 z_5^2\right), \tag{5.12}$$

where

$$P_1 = c_1 - A^2 - B^2 - \frac{1}{2}\mu_1^2 > 0,$$
$$P_2 = \frac{1}{2}\mu_2^2 - D^2 - E^2 - c_4 > 0,$$
$$P_3 = c_5 - \frac{1}{2} - F^2 - G^2 - q - \frac{1}{2}\mu_3^2 > 0,$$
$$P_4 = \nu - c_6 - H^2 - \frac{1}{2} + \frac{1}{2}\mu_4^2 > 0,$$
$$P_5 = d - 3c_7 + 2\mu_5^2 - I^2 - \frac{1}{2} > 0.$$

Define $\Phi = \min\{P_1, P_2, P_3, P_4, P_5\}$, ensuring that $\Phi > 0$. With this definition, Eq (5.12) can be expressed as $LU \leq -\Phi|z(t)|^2$. Therefore, inequality (5.4) holds, indicating that the trivial solution of model (5.1) possesses asymptotic mean square stability. □

Remark 5.1. *Theorem 5.1 shows that when μ_i is sufficiently small, under the influence of random fluctuations (such as environmental changes, policy adjustments, or randomness in disease transmission), the spread of infectious diseases like influenza will gradually stabilize and will not experience uncontrolled outbreaks or extinction due to random disturbances.*

To better understand the dynamic differences between the deterministic and stochastic models, we perform numerical simulations of the stochastic model using the Euler-Maruyama discretization scheme. The resulting phase-space trajectories and associated statistical characteristics are presented in Figures 14–16. In Figure 14, the initial conditions are set as $[12; 3; 6; 8; 12]$, and the parameters are chosen as $u = 0.8$, $\mu_1 = 0.8$, $\mu_2 = 0.89$, $\mu_3 = 0.75$, $\mu_4 = 0.87$, and $\mu_5 = 0.9$. Under the condition $R_0 > \phi$, the solution of the deterministic model converges to an EE point $P^* = (9.43976, 47.4031, 0.185743, 2.74881, 1.47851)$, indicating that in the absence of stochastic perturbations, influenza will persist at this equilibrium state over the long term. However, when stochastic perturbations with intensities μ_i are introduced, the system trajectories no longer stabilize at P^* but instead exhibit sustained fluctuations around it. To characterize these stochastic dynamics, we simulat the stationary probability density functions of the state variables. The results show that the solution of the stochastic model is primarily concentrated around P^*, with the peak of the solution corresponding to the location of the deterministic equilibrium in the figure. This indicates that, even in the presence of environmental noise, the disease fluctuates around the EE level than completely disappearing or leading to large-scale outbreaks.

Furthermore, to investigate the effect of the influenza mortality rate (u) on the stochastic model, Figure 15 modifies the parameters from the conditions in Figure 14, reducing u from 0.8 to 0.2. The numerical results show that as u decreases, the dynamic behavior of the stochastic model exhibits significantly less randomness and fluctuation over time. This change suggests that during an influenza outbreak, if sufficient medical conditions are in place and appropriate control measures are implemented promptly, the impact of external random factors on the disease's spread can be significantly reduced, leading to more stable epidemic dynamics. This further emphasizes the importance of taking swift and effective intervention measures early in an outbreak to reduce uncertainty and optimize control outcomes.

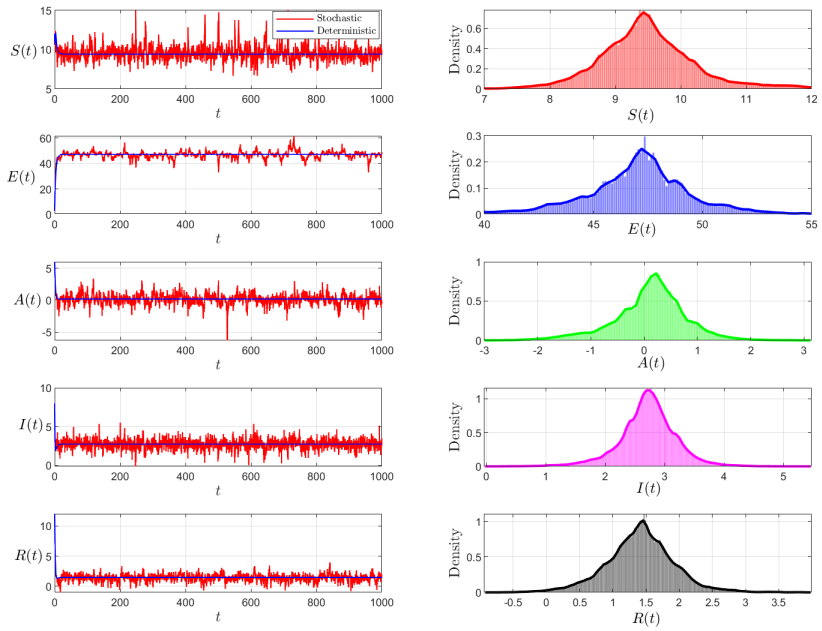

Figure 14. Dynamical behavior of model (2.2) and histograms with probability density functions of state variables. Initial values [12, 3, 6, 8, 12], with fixed parameters $\beta = 0.8, d = 0.16, k = 0.024, \alpha = 0.3, \sigma = 0.6, p = 0.2, q = 0.13, \Lambda = 12, \delta = 0.08, \nu = 0.4, u = 0.8, \mu_1 = 0.8, \mu_2 = 0.89, \mu_3 = 0.75, \mu_4 = 0.87$, and $\mu_5 = 0.9$.

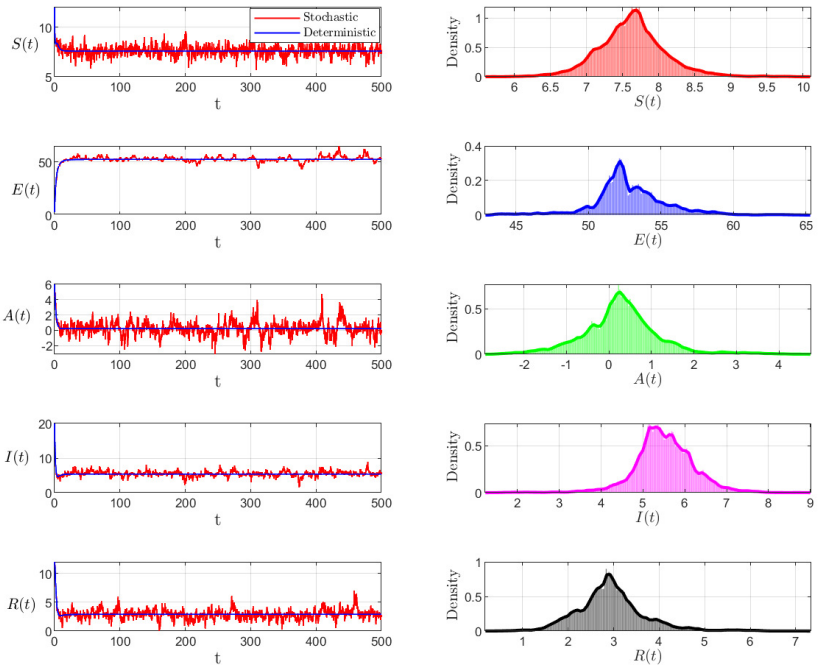

Figure 15. Dynamical behavior of model (2.2) and histograms with probability density functions of state variables. Parameters: $u = 0.2$. Other parameters are the same as in Figure 14.

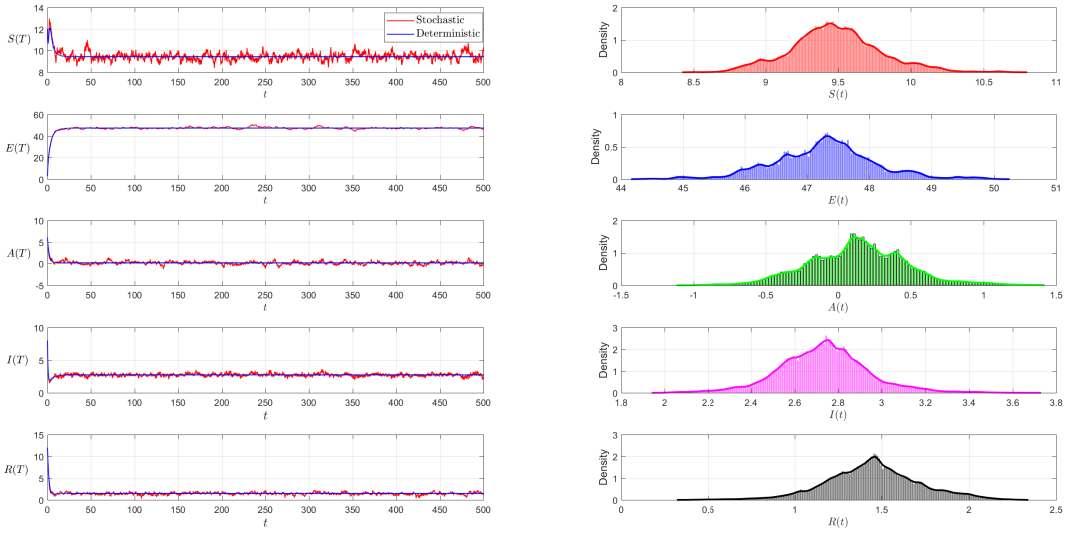

Figure 16. Dynamical behavior of model (2.2) and histograms with probability density functions of state variables. Parameters: $\mu_1 = 0.4, \mu_2 = 0.4, \mu_3 = 0.4, \mu_4 = 0.4$, and $\mu_5 = 0.4$. Other parameters are the same as in Figure 14.

Furthermore, to analyze the effect of different stochastic intensities μ_i on the dynamics of model (5.1), we keep all other conditions from Figure 14 unchanged, except for reducing all μ_i to 0.4. By comparing Figures 14 and 16, we observe that when the stochastic intensity is reduced, the influence of random factors on the dynamics of model (5.1) also decreases. This will aid in the control of influenza, meaning that if an outbreak occurs, timely and appropriate control measures by the relevant authorities, along with active public cooperation, will significantly increase the chances of controlling the influenza outbreak.

6. Real data example

Parameter estimation (PE) plays a vital role in validating the rationality of influenza transmission models. The spread of influenza involves a variety of complex biological mechanisms, and accurately abstracting these processes into mathematical models is inherently challenging. Through PE, key model parameters can be determined based on real epidemiological data within a reasonable range, thereby enhancing the model's ability to capture the dynamics of influenza transmission. Accurate parameter estimation not only improves the predictive accuracy of the model but also helps uncover the underlying mechanisms of influenza spread, providing a scientific basis and decision support for the formulation and optimization of control strategies.

In this section, we use four sets of real influenza-related data: (1) Global weekly B-type influenza cases from week 21 to week 52 of 2021 [53]; (2) the number of positive A-type influenza specimens in the United States from week 21 to week 52 of 2023 [54]; (3) global weekly A-type influenza cases from week 21 to week 52 of 2021 [53]; and (4) confirmed A(H1N1) influenza cases registered in the Bogotá metropolitan area of Colombia from week 17 to week 44 of 2009 [55]. The model parameters

in model (2.2) are fitted using the least squares method, with the fitting results shown in Figure 17 and the corresponding parameter values listed in Table 3.

Table 3. Model (2.2) obtains the corresponding parameter values through fitting with four sets of real data.

Parameter	Value (1)	Value (2)	Value (3)	Value (4)	Source
Λ	5.955913563771e+6	6.403864744384e+6	5.710931527482e+6	9.18806417e+2	Fitted
β	7.322600000000e-2	1.050110000000e-1	8.641400000000e-2	2.16000000e-4	Fitted
α	7.372409500000e+1	1.613820220000e+2	1.019088640000e+2	1.00000000e-6	Fitted
d	2.000000000000e-6	4.000000000000e-6	1.000000000000e-6	1.00000000e-6	Fitted
σ	3.013700000000e-2	4.577140000000e-1	2.729020000000e-1	1.00000000e-6	Fitted
δ	1.560000000000e-4	1.230000000000e-4	2.160000000000e-4	9.98558000e-1	Fitted
k	8.999920000000e-1	8.996340000000e-1	8.994210000000e-1	9.00000000e-1	Fitted
p	1.563700000000e-2	1.681800000000e-2	1.764300000000e-2	1.30000000e-5	Fitted
q	1.100000000000e-5	3.873300000000e-2	7.720000000000e-4	9.98376000e-1	Fitted
γ	3.416000000000e-2	2.895300000000e-2	1.000000000000e-6	9.99956000e-1	Fitted
u	3.931500000000e-2	3.486500000000e-2	1.000000000000e-6	9.99957000e-1	Fitted
η	7.787120000000e-1	8.337560000000e-1	7.839580000000e-1	9.85700000e-1	Fitted
$S(0)$	1.000000000000e+5	1.000000000000e+5	1.000000000000e+5	1.00000000e+5	Assumed
$E(0)$	1.000000000000e+3	5.000000000000e+2	5.000000000000e+2	5.00000000e+1	Assumed
$A(0)$	6.000000000000e+2	3.000000000000e+2	3.000000000000e+2	5.00000000e+1	Assumed
$I(0)$	5.130000000000e+2	4.100000000000e+1	6.300000000000e+1	4.00000000e+0	Assumed
$R(0)$	4.000000000000e+2	2.000000000000e+1	5.000000000000e+1	3.00000000e+0	Assumed

As shown in Figure 17, the model fits all four datasets well, demonstrating strong explanatory power. Moreover, in all best-fitting scenarios, the fractional-order parameter η is not equal to 1, indicating that the fractional-order differential model can better capture the complexity of influenza transmission. This allows for more accurate predictions of future case numbers and provides deeper insight into the underlying transmission mechanisms.

To further analyze the specific development trends of influenza and the impact of different η values on the model dynamics, we incorporate the parameters fitted from model (2.2) into the model for simulation. Specifically, we use the parameters fitted from the 2021 week 21 to week 52 global B-type influenza case data and the 2009 Bogotá metropolitan area H1N1 influenza confirmed cases data from week 17 to week 44 in Colombia, then apply FDE12 to plot the time series of each variable, as shown in Figures 18 and 19.

From Figure 18, it can be observed that global A-type influenza cases will continue to rise in the coming weeks. In Figure 19, it can be seen that in the following weeks, the influenza cases in Bogotá will fluctuate and gradually stabilize over time. Further analysis of Figure 18 reveals that when η exceeds the optimal fitted parameter value, the influenza control strategy faces issues. In the early stages of the outbreak, an overly high η results in excessive government investment, leading to resource waste. During the middle phase, insufficient investment may cause ineffective control, potentially resulting in the failure of influenza control. As shown in Figure 4, under different η values, each peak and trough in model (2.2) varies. This means that using inappropriate parameters to guide influenza control could lead to resource waste at best, or, at worst, trigger an influenza outbreak.

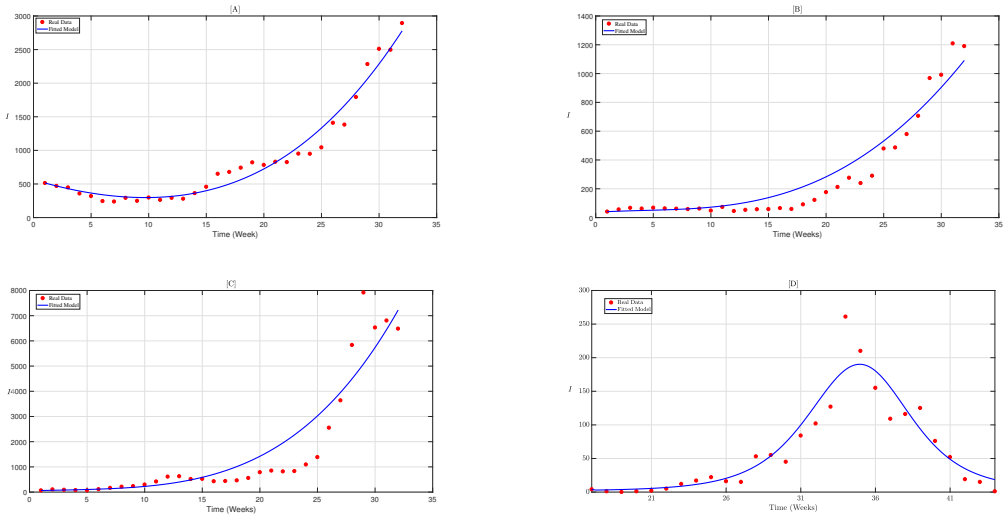

Figure 17. The fitting curves of model (2.2) with real influenza case data. [A] represents the fitting curve of model (2.2) with real global influenza B case data from 2021 (weeks 21 to 52), [B] represents the fitting curve of model (2.2) with real influenza A positive specimens in the U.S. from 2023 (weeks 21 to 52), [C] represents the fitting curve of model (2.2) with real global influenza A case data from 2021 (weeks 21 to 52), and [D] represents the fitting curve of model (2.2) with real confirmed H1N1 influenza A cases in the Bogotá Metropolitan Area, Colombia (weeks 17 to 44, 2009).

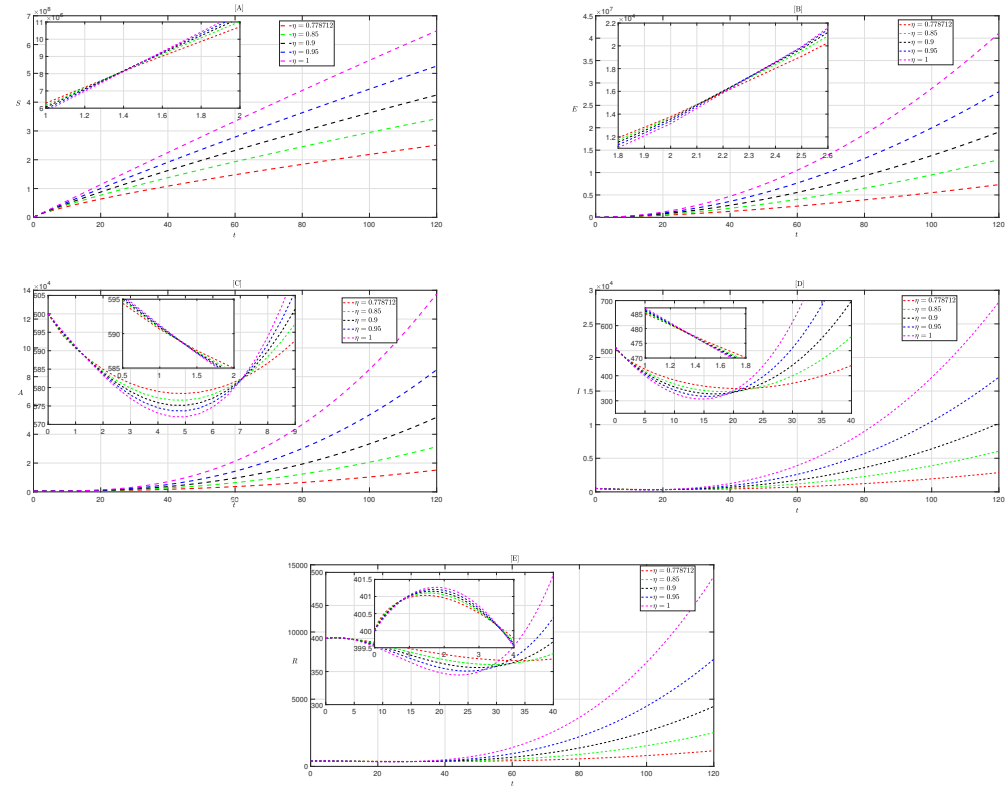

Figure 18. The dynamics of model (2.2) under different η values with the remaining parameters fixed to those obtained from fitting with the 2021 global influenza B cases from weeks 21 to 52.

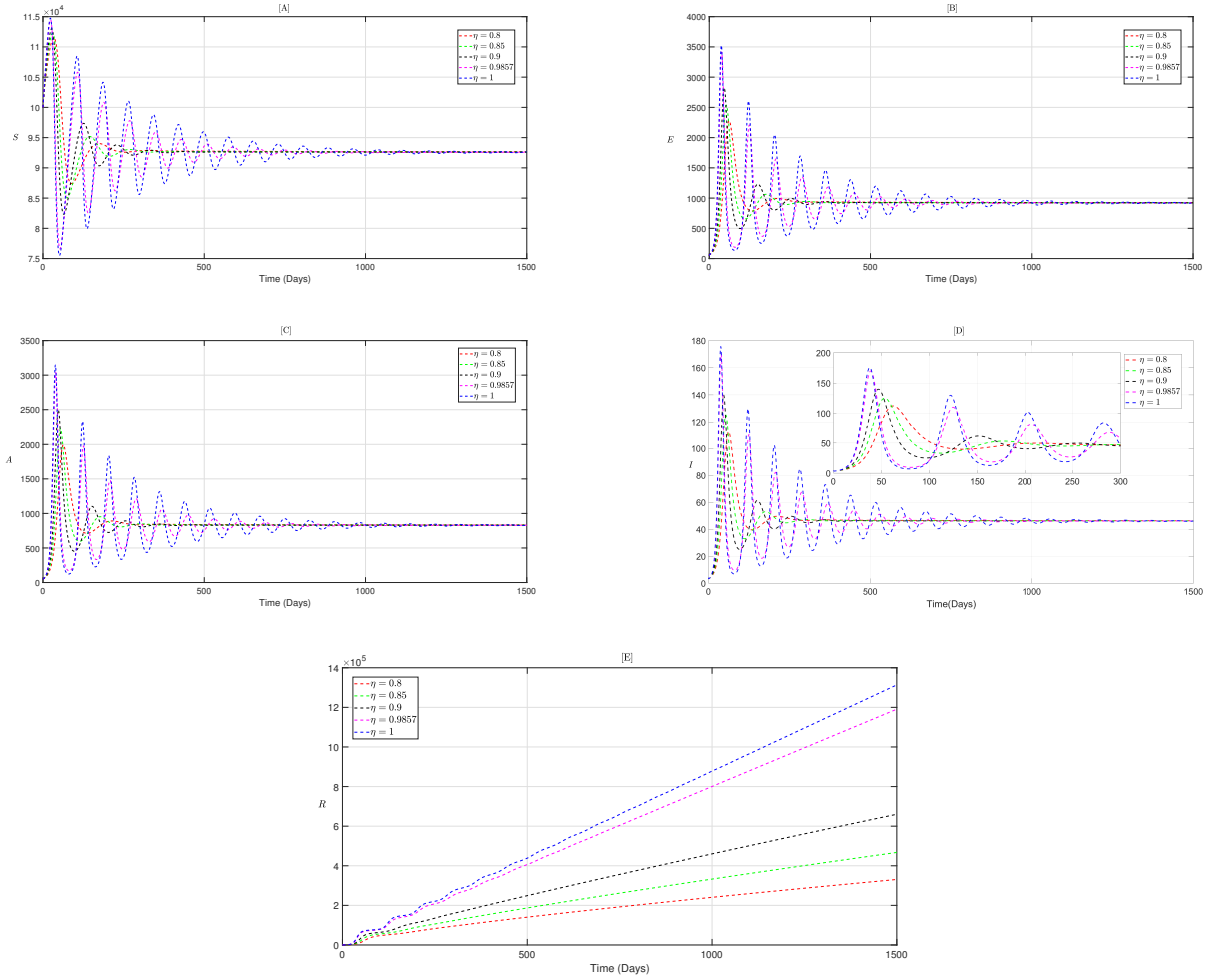

Figure 19. The dynamics of model (2.2) at different η values, with the other parameters fixed to the values fitted from the number of reported confirmed H1N1 influenza cases in the Bogotá Metropolitan Area, Colombia, from week 17 to week 44 in 2009.

7. Discussion and conclusions

In this study, we proposed a fractional-order SEAIR influenza model to analyze the transmission dynamics of influenza. First, the existence, uniqueness, and non-negativity of the solution to model (2.2) are proved, ensuring the model's biological relevance. Then, the existence and stability of the equilibrium points of model (2.2) are analyzed, and the expression for the basic reproduction number (R_0) is calculated. The study finds that the outbreak of influenza is not solely determined by the simple relationship between R_0 and 1. Specifically, when $R_0 < \phi$, model (2.2) has a locally asymptotically stable DFE point P_0; when $R_0 > \phi$, model (2.2) has a globally asymptotically stable EE point P^* and an unstable disease-free equilibrium point P_0. This suggests that if $R_0 < \phi$, the influenza will naturally fade without the need for control strategies; however, when $R_0 > \phi$, the influenza will outbreak and cannot be controlled through natural processes. Therefore, the key to controlling influenza lies in making $R_0 < \phi$.

Subsequently, to further assess the importance of different parameters in the influenza transmission process, we calculated the normalized forward sensitivity indices of the variables in model (2.2). This helps identify the parameters that have the greatest impact on influenza transmission. The results show that the inflow rate of susceptible individuals (Λ), the effective contact rate between symptomatic infecteds and susceptibles (β), and the natural death rate (d) have the greatest sensitivity in model (2.2), indicating that these three parameters play a key role in the spread of influenza. Therefore, in subsequent control strategies, the focus should be on adjusting these parameters, such as reducing Λ by restricting population movement, decreasing β through enhanced isolation measures, and lowering the death rate (d) by improving public health measures, to effectively control the spread of influenza.

To further explore the specific effects of Λ, β, and d on the dynamics of model (2.2), we conducted a bifurcation analysis. We found that model (2.2) undergoes a bifurcation of equilibrium points and a transcritical bifurcation when $R_0 = \phi$. To validate the theoretical analysis, we performed numerical simulations and plotted the bifurcation diagrams with Λ and β as bifurcation parameters (as shown in Figure 7), as well as the transcritical bifurcation diagrams with β and d as bifurcation parameters (as shown in Figure 8). From Figure 7, it can be seen that when Λ is sufficiently small, an increase in β does not lead to an influenza outbreak, indicating that controlling the inflow and outflow of the population in a region is an effective preventive measure. From Figure 8, it can be seen that when β is sufficiently small, the influenza will not outbreak, further emphasizing the importance of control measures such as home isolation and wearing masks in influenza prevention.

Considering the importance of control strategies such as early isolation and vaccination in influenza control, we developed an influenza model (4.1) that incorporates these control strategies. Subsequently, using optimal control theory, we proved the existence of an optimal solution for model (4.1) and derived the expression for the optimal solution. To further analyze the impact of initial values and the parameter η on control effectiveness, we conducted a numerical analysis using the particle swarm optimization algorithm, examining how different initial values and the parameter η affect the control intensity, the size of the objective function, and the dynamic changes of state variables. We found that as the population size and η increase, the required maximum control duration and treatment costs also increase. This indicates that limiting population movement and implementing home isolation measures are crucial during an influenza outbreak. This also highlights the importance of developing more scientifically sound and reasonable influenza models. Only by accurately predicting the development trends of influenza can its spread be effectively controlled without unnecessary economic waste.

Moreover, the spread of influenza is accompanied by significant randomness. Therefore, based on model (2.2), we introduced a small perturbation around the EE point and assumed that these perturbations are proportional to the deviations of $S(t)$, $E(t)$, $A(t)$, $I(t)$, and $R(t)$, thus establishing a stochastic influenza model (5.1). Using stochastic process theory, we proved the conditions for P-index stability and mean-square stability of model (5.1). Then, we conducted a numerical analysis to study the impact of the fatality rate of the influenza virus on the randomness factors. We found that as the fatality rate of the virus decreases, the impact of random factors on the spread of influenza diminishes. This indicates that with timely control strategies and improved medical standards, influenza will be more easily and effectively controlled.

In addition, to validate the effectiveness and universality of model (2.2), we used four sets of real influenza-related data and fitted the corresponding parameter values using the least squares method, visualizing the optimal curve as shown in Figure 17. From the figure, it can be seen that the fitting result

is quite good, indicating that model (2.2) has a certain reference value for future influenza predictions. Furthermore, we observed that the fitted parameter η values are all less than 1, which suggests that the fractional-order influenza model can better adapt to the complex transmission dynamics of influenza. Subsequently, we substituted two sets of fitted parameters into model (2.2) and used numerical analysis to predict the future dynamics of influenza spread, as shown in Figures 18 and 19. From Figure 18, it can be observed that the number of global influenza cases may continue to increase in the coming weeks, while Figure 19 indicates that the number of influenza cases in the Bogotá metropolitan area of Colombia will exist in the coming weeks but will decrease and show significant fluctuations.

Finally, considering that the spread of influenza is influenced by various factors such as seasonal changes, age structure, spatial dynamics, and potential delays in reported data, these aspects have not been addressed in the current study. Therefore, in future research, we focus on incorporating these factors into the model to improve its accuracy and applicability. Additionally, we plan to further refine optimal control theory in future work and explore innovative control strategies to better address the challenges of influenza transmission. By doing so, we aim to make the model more comprehensive in reflecting the complexities of influenza transmission, thereby providing scientific guidance for the development of more precise intervention strategies and treatment plans. Furthermore, analyzing these factors will help improve the timeliness and accuracy of influenza predictions, offering stronger support for global influenza control efforts.

Author contributions

Hanyun Zhang: Review Editing; Guoqin Chen: Writing; Xingxiao Wu: Software; Yanfang Zhao and Yujiao Wang: Idea, Methodology, Formal analysis, Project Administration. Hanyun Zhang, Guoqin Chen and Xingxiao Wu contributed equally to this work and are considered co-first authors. Yanfang Zhao and Yujiao Wang are the corresponding authors. All authors read and approved the final manuscript.

Use of Generative-AI tools declaration

The authors declare they have not used Artificial Intelligence (AI) tools in the creation of this article.

Acknowledgments

This work was supported in the Yunnan Province International Joint Laboratory for Intelligent Integration and Application of Ethnic Multilingualism (202403AP140014).

Data availability statement

The data used for numerical simulation in this study are sourced from references [53–55], and these data are publicly available, making them accessible for use.

Conflict of interest

The authors declare that there are no conflicts of interest regarding the publication of this paper.

References

1. E. C. Hutchinson, Influenza virus, *Trends Microbiol.*, **26** (2018), 809–810. https://doi.org/10.1016/j.tim.2018.05.013
2. A. Jutel, E. Banister, "I was pretty sure I had the 'flu": qualitative description of confirmed-influenza symptoms, *Soc. Sci. Med.*, **99** (2013), 49–55. https://doi.org/10.1016/j.socscimed.2013.10.011
3. A. Trilla, G. Trilla, C. Daer, The 1918 "spanish flu" in Spain, *Clin. Infect. Dis.*, **47** (2008), 668–673. https://doi.org/10.1086/590567
4. W. Barclay, P. Openshaw, The 1918 influenza pandemic: one hundred years of progress, but where now? *Lancet Resp. Med.*, **6** (2018), 588–589. https://doi.org/10.1016/S2213-2600(18)30272-8
5. J. Dunning, R. S. Thwaites, P. J. M. Openshaw, Seasonal and pandemic influenza: 100 years of progress, still much to learn, *Mucosal Immunol.*, **13** (2020), 566–573. https://doi.org/10.1038/s41385-020-0287-5
6. R. Casagrandi, L. Bolzoni, S. A. Levin, V. Andreasen, The SIRC model and influenza A, *Math. Biosci.*, **200** (2006), 152–169. https://doi.org/10.1016/j.mbs.2005.12.029
7. K. M. Mohammad, A. A. Akhi, Md. Kamrujjaman, Bifurcation analysis of an influenza A (H1N1) model with treatment and vaccination, *PloS One*, **20** (2025), e0315280. https://doi.org/10.1371/journal.pone.0315280
8. C. Andreu-Vilarroig, G. González-Parra, R. J. Villanueva, Mathematical modeling of influenza dynamics: integrating seasonality and gradual waning immunity, *Bull. Math. Biol.*, **87** (2025), 75. https://doi.org/10.1007/s11538-025-01454-w
9. J. Z. Ndendya, L. Leandry, A. M. Kipingu, A next-generation matrix approach using Routh–Hurwitz criterion and quadratic Lyapunov function for modeling animal rabies with infective immigrants, *Healthcare Anal.*, **4** (2023), 100260. https://doi.org/10.1016/j.health.2023.100260
10. J. Z. Ndendya, Y. A. Liana, A deterministic mathematical model for conjunctivitis incorporating public health education as a control measure, *Model. Earth Syst. Environ.*, **11** (2025), 216. https://doi.org/10.1007/s40808-025-02393-0
11. J. Z. Ndendya, J. A. Mwasunda, S. Edward, N. Shaban, A fractional-order model for rabies transmission dynamics using the Atangana–Baleanu–Caputo derivative and MCMC methods, *Sci. Afr.*, **29** (2025), e02800. https://doi.org/10.1016/j.sciaf.2025.e02800
12. M. A. Bahloul, A. Chahid, T. M. Laleg-Kirati, Fractional-order SEIQRDP model for simulating the dynamics of COVID-19 epidemic, *IEEE Open J. Eng. Med. Biol.*, **1** (2020), 249–256. https://doi.org/10.1109/OJEMB.2020.3019758
13. A. Mahata, S. Paul, S. Mukherjee, M. Das, B. Roy, Dynamics of caputo fractional order SEIRV epidemic model with optimal control and stability analysis, *Int. J. Appl. Comput. Math.*, **8** (2022), 28. https://doi.org/10.1007/s40819-021-01224-x

14. B. Mohammadaliee, M. E. Samei, V. Roomi, S. Rezapour, Optimal control strategies and cost-effectiveness analysis for infectious diseases under fractal-fractional derivative: a case study of Cholera outbreak, *J. Appl. Math. Comput.*, **71** (2025), 4197–4226. https://doi.org/10.1007/s12190-024-02331-w

15. C. T. Deressa, G. F. Duressa, Analysis of Atangana–Baleanu fractional-order SEAIR epidemic model with optimal control, *Adv. Differ. Equ.*, **2021** (2021), 174. https://doi.org/10.1186/s13662-021-03334-8

16. S. Soulaimani, A. Kaddar, Analysis and optimal control of a fractional order SEIR epidemic model with general incidence and vaccination, *IEEE Access*, **11** (2023), 81995–82002. https://doi.org/10.1109/ACCESS.2023.3300456

17. I. Malmir, New pure multi-order fractional optimal control problems with constraints: QP and LP methods, *ISA Trans.*, **153** (2024), 155–190. https://doi.org/10.1016/j.isatra.2024.08.003

18. N. P. Dong, H. V. Long, A. Khastan, Optimal control of a fractional order model for granular SEIR epidemic with uncertainty, *Commun. Nonlinear Sci. Numer. Simul.*, **88** (2020), 105312. https://doi.org/10.1016/j.cnsns.2020.105312

19. Y. Zhao, T. Li, R. Kang, X. He, Dynamical analysis of a novel fractional order SIDARTHE epidemic model of COVID-19 with the Caputo–Fabrizio (CF) derivative, *Adv. Cont. Discr. Mod.*, **2024** (2024), 3. https://doi.org/10.1186/s13662-024-03798-4

20. C. N. Angstmann, B. I. Henry, A. V. McGann, A fractional-order infectivity SIR model, *Phys. A*, **452** (2016), 86–93. https://doi.org/10.1016/j.physa.2016.02.029

21. C. N. Angstmann, A. M. Erickson, B. I. Henry, A. V. McGann, J. M. Murray, J. A. Nichols, A general framework for fractional order compartment models, *SIAM Rev.*, **63** (2021), 375–392. https://doi.org/10.1137/21M1398549

22. S. Momani, A. Freihat, M. Alabedalhadi, M. Al-Smadi, S. Al-Omari, Investigation of numerical solutions for a fractional seasonal influenza model in deterministic environments, *Math. Meth. Appl. Sci.*, **48** (2025), 10602–10615. https://doi.org/10.1002/mma.10905

23. J. Lamwong, P. Pongsumpun, Optimal control and stability analysis of influenza transmission dynamics with quarantine interventions, *Model. Earth Syst. Environ.*, **11** (2025), 233. https://doi.org/10.1007/s40808-025-02413-z

24. J. Yang, L. Yang, Z. Jin, Optimal strategies of the age-specific vaccination and antiviral treatment against influenza, *Chaos Soliton. Fract.*, **168** (2023), 113199. https://doi.org/10.1016/j.chaos.2023.113199

25. Y. Chen, J. Zhang, Z. Jin, Optimal control of an influenza model with mixed cross-infection by age group, *Math. Comput. Simul.*, **206** (2023), 410–436. https://doi.org/10.1016/j.matcom.2022.11.019

26. J. Xiao, P. Yu, Z. Zhang, Weighted composite asymmetric Huber estimation for partial functional linear models, *AIMS Math.*, **7** (2022), 7657–7684. https://doi.org/10.3934/math.2022430

27. J. Moon, The Pontryagin type maximum principle for Caputo fractional optimal control problems with terminal and running state constraints, *AIMS Math.*, **10** (2025), 884–920. https://doi.org/10.3934/math.2025042

28. C. J. Song, Y. Zhang, Conserved quantities for Hamiltonian systems on time scales, *Appl. Math. Comput.*, **313** (2017), 24–36. https://doi.org/10.1016/j.amc.2017.05.074

29. E. M. Farah, S. Amine, S. Ahmad, K. Nonlaopon, K. Allali, Theoretical and numerical results of a stochastic model describing resistance and non-resistance strains of influenza, *Eur. Phys. J. Plus*, **137** (2022), 1169. https://doi.org/10.1140/epjp/s13360-022-03302-5

30. T. Su, X. Zhang, Y. Kao, D. Jiang, Dynamical analysis and numerical simulation of a stochastic influenza transmission model with human mobility and ornstein-uhlenbeck process, *Qual. Theory Dyn. Syst.*, **24** (2025), 64. https://doi.org/10.1007/s12346-025-01226-w

31. A. Khan, R. Ikram, A. Saeed, M. Zahri, T. Gul, U. W. Humphries, Extinction and persistence of a stochastic delayed Covid-19 epidemic model, *Comput. Meth. Biomech. Biomed. Eng.*, **26** (2023), 424–437. https://doi.org/10.1080/10255842.2022.2065631

32. L. Basnarkov, SEAIR epidemic spreading model of COVID-19, *Chaos Soliton. Fract.*, **142** (2021), 110394. https://doi.org/10.1016/j.chaos.2020.110394

33. A. A. Khan, R. Amin, S. Ullah, W. Sumelka, M. Altanji, Numerical simulation of a Caputo fractional epidemic model for the novel coronavirus with the impact of environmental transmission, *Alex. Eng. J.*, **61** (2022), 5083–5095. https://doi.org/10.1016/j.aej.2021.10.008

34. M. Amouch, N. Karim, Fractional-order mathematical modeling of COVID-19 dynamics with different types of transmission, *Numer. Algebra Control Optim.*, **15** (2025), 386–415. https://doi.org/10.3934/naco.2023019

35. K. Diethelm, Monotonicity of functions and sign changes of their Caputo derivatives, *Fract. Calculus Appl. Anal.*, **19** (2016), 561–566. https://doi.org/10.1515/fca-2016-0029

36. H. L. Li, L. Zhang, C. Hu, Y. L. Jiang, Z. Teng, Dynamical analysis of a fractional-order predator-prey model incorporating a prey refuge, *J. Appl. Math. Comput.*, **54** (2017), 435–449. https://doi.org/10.1007/s12190-016-1017-8

37. E. Ahmed, A. S. Elgazzar, On fractional order differential equations model for nonlocal epidemics, *Phys. A*, **379** (2007), 607–614. https://doi.org/10.1016/j.physa.2007.01.010

38. W. Qin, S. Zhang, Y. Yang, J. Zhang, A discrete SIR epidemic model incorporating media impact, resource limitaions and threshold switching strategies, *Infect. Dis. Model.*, **10** (2025), 1270–1290. https://doi.org/10.1016/j.idm.2025.07.006

39. Y. Li, Y. Q. Chen, I. Podlubny, Stability of fractional-order nonlinear dynamic systems: Lyapunov direct method and generalized Mittag–Leffler stability, *Comput. Math. Appl.*, **59** (2010), 1810–1821. https://doi.org/10.1016/j.camwa.2009.08.019

40. P. Van den Driessche, J. Watmough, Reproduction numbers and sub-threshold endemic equilibria for compartmental models of disease transmission, *Math. Biosci.*, **180** (2002), 29–48. https://doi.org/10.1016/S0025-5564(02)00108-6

41. E. Ahmed, A. M. A. El-Sayed, H. A. A. El-Saka, On some Routh–Hurwitz conditions for fractional order differential equations and their applications in Lorenz, Rössler, Chua and Chen systems, *Phys. Lett. A*, **358** (2006), 1–4. https://doi.org/10.1016/j.physleta.2006.04.087

42. J. Huo, H. Zhao, L. Zhu, The effect of vaccines on backward bifurcation in a fractional order HIV model, *Nonlinear Anal.*, **26** (2015), 289–305. https://doi.org/10.1016/j.nonrwa.2015.05.014

43. H. Delavari, D. Baleanu, J. Sadati, Stability analysis of Caputo fractional-order nonlinear systems revisited, *Nonlinear Dyn.*, **67** (2012), 2433–2439. https://doi.org/10.1007/s11071-011-0157-5
44. J. Z. Ndendya, J. A. Mwasunda, N. S. Mbare, Modeling the effect of vaccination, treatment and public health education on the dynamics of norovirus disease, *Model. Earth Syst. Environ.*, **11** (2025), 150. https://doi.org/10.1007/s40808-025-02326-x
45. J. Z. Ndendya, E. Mureithi, J. A. Mwasunda, G. Kagaruki, N. Shaban, M. Mayige, Modelling the effects of quarantine and protective interventions on the transmission dynamics of Marburg virus disease, *Model. Earth Syst. Environ.*, **11** (2025), 81. https://doi.org/10.1007/s40808-024-02264-0
46. J. Guckenheimer, P. Holmes, *Nonlinear oscillations, dynamical systems, and bifurcations of vector fields*, Springer Science & Business Media, 2013.
47. S. Majee, S. Jana, T. K. Kar, S. Barman, D. K. Das, Modeling and analysis of Caputo-type fractional-order SEIQR epidemic model, *Int. J. Dyn. Control, **12** (2024), 148–166.* https://doi.org/10.1007/s40435-023-01348-6
48. X. Yang, A note on Hölder inequality, *Appl. Math. Comput.*, **134** (2003), 319–322. https://doi.org/10.1016/S0096-3003(01)00286-7
49. L. S. Pontryagin, *Mathematical theory of optimal processes*, 1 Ed., Routledge, 2018. https://doi.org/10.1201/9780203749319
50. J. Z. Ndendya, G. Mlay, H. Rwezaura, Mathematical modelling of COVID-19 transmission with optimal control and cost-effectiveness analysis, *Comput. Meth. Prog. Biomed. Update*, **5** (2024), 100155. https://doi.org/10.1016/j.cmpbup.2024.100155
51. A. Lahrouz, L. Omari, D. Kiouach, Global analysis of a deterministic and stochastic nonlinear SIRS epidemic model, *Nonlinear Anal.*, **16** (2011), 59–76. https://doi.org/10.15388/NA.16.1.14115
52. V. N. Afanasiev, V. Kolmanovskii, V. R. Nosov, *Mathematical theory of control systems design*, Springer Science & Business Media, 2013.
53. Statista, Reported cases of influenza per week in 2021 worldwide, by type, accessed on July 27, 2025. Available from: `https://www.statista.com/statistics/1120860/influenza-cases-worldwide-type-week/`.
54. Statista, Number of specimens testing positive for influenza in the United States in 2024, by week and subtype/lineage, accessed on July 27, 2025. Available from: `https://www.statista.com/statistics/1122427/influenza-cases-number-us-by-subtype-week/`.
55. G. González-Parra, A. J. Arenas, B. M. Chen, A fractional order epidemic model for the simulation of outbreaks of influenza A(H1N1), *Math. Meth. Appl. Sci.*, **37** (2024), 2218–2226. https://doi.org/10.1002/mma.2968

AIMS Press